This paper is available on line at http://www.mcponline.org

BioID-based Identification of Skp Cullin F-box (SCF)$^{\beta\text{-TrCP1/2}}$ E3 Ligase Substrates*[S]

Etienne Coyaud‡¶¶, Monika Mis§¶¶, Estelle M. N. Laurent‡, Wade H. Dunham¶, Amber L. Couzens¶, Melanie Robitaille§, Anne-Claude Gingras¶‖, Stephane Angers§, and Brian Raught‡ ‡‡§§**

The identification of ubiquitin E3 ligase substrates has been challenging, due in part to low-affinity, transient interactions, the rapid degradation of targets and the inability to identify proteins from poorly soluble cellular compartments. SCF$^{\beta\text{-TrCP1}}$ and SCF$^{\beta\text{-TrCP2}}$ are well-studied ubiquitin E3 ligases that target substrates for proteasomal degradation, and play important roles in Wnt, Hippo, and NFκB signaling. Combining 26S proteasome inhibitor (MG132) treatment with proximity-dependent biotin labeling (BioID) and semiquantitative mass spectrometry, here we identify SCF$^{\beta\text{-TrCP1/2}}$ interacting partners. Based on their enrichment in the presence of MG132, our data identify over 50 new putative SCF$^{\beta\text{-TrCP1/2}}$ substrates. We validate 12 of these new substrates and reveal previously unsuspected roles for β-TrCP in the maintenance of nuclear membrane integrity, processing (P)-body turnover and translational control. Together, our data suggest that β-TrCP is an important hub in the cellular stress response. The technique presented here represents a complementary approach to more standard IP-MS methods and should be broadly applicable for the identification of substrates for many ubiquitin E3 ligases. ***Molecular & Cellular Proteomics 14: 10.1074/mcp.M114.045658, 1781–1795, 2015.***

More than 600 putative ubiquitin E3 ligases are encoded in the human genome (1, 2). Although a number of these proteins are known to play critical roles in human health (1–4), the specific biological functions—and substrates—of most E3s remain poorly characterized. The identification of E3 substrates has been difficult in part because: (1) ligase - substrate interactions are often of low affinity (generally in the high nM to microMolar (μM) range) and/or of a transient nature; (2) many substrates are subjected to rapid proteasomal degradation and are therefore not available for detection; (3) the human ubiquitome is extremely complex, and; (4) many substrate proteins are localized to poorly soluble cellular compartments, making their isolation and identification by standard immunoprecipitation (IP)-based techniques extremely challenging (1–4).

Methods such as protein chip (5) and yeast two-hybrid screening (6) have been used to identify a limited number of E3-substrate interactions. However, these methods are not conducted in live mammalian cells, and may not be generally applicable for the identification of substrates of the hundreds of unique multi-protein E3 complexes (*e.g.* SCF, APC, VHL, *etc.*) or the identification of E3-substrate interactions that are dependent on specific types of post-translational modifications. Several putative inhibitors of apoptosis substrates were identified using the recently described NEDDylator technique (7), in which the E2 protein UBC12 (UBE2M) is fused to the E3 ligase of interest, allowing for the conjugation of the ubiquitin-like protein NEDD8 to substrates. Global protein stability profiling (8) and quantitative mass spectrometry methods (9) have also been used successfully to identify E3 targets. However, because of their cost and/or complexity, and the challenges posed by the extremely large size of the human ubiquitome, these methods have not been widely adopted to date.

Proximity-based biotinylation, or BioID[1] (10), is a new method developed for the characterization of protein-protein interactions in living cells. Briefly, a protein of interest is fused in-frame with an *E. coli* biotin conjugating enzyme mutant (BirA R118G, or BirA*). The BirA* moiety can efficiently activate biotin, but exhibits a reduced affinity for the activated molecule (11); biotinoyl-AMP thus simply diffuses away from BirA* and reacts with nearby amine groups - including those present on lysine residues in neighboring polypeptides. Following cell lysis, biotinylated proteins can be affinity purified using streptavidin and identified using mass spectrometry

From the ‡Princess Margaret Cancer Centre, University Health Network; §Department of Pharmaceutical Sciences, Leslie Dan Faculty of Pharmacy, University of Toronto; ¶Lunenfeld-Tanenbaum Research Institute, Mount Sinai Hospital; ‖Department of Molecular Genetics, University of Toronto; **Department of Biochemistry, University of Toronto; ‡‡Department of Medical Biophysics, University of Toronto, Toronto, ON Canada

Received October 15, 2014, and in revised form, April 1, 2015

Published, MCP Papers in Press, April 21, 2015, DOI 10.1074/mcp.M114.045658

Author contributions: EC and MM conducted the experiments; EMNL and MR built constructs and cell lines; WHD and ALC provided constructs and cell lines under the guidance of A-CG; SA and BR conceived the project and designed the experiments. BR wrote the manuscript.

[1] The abbreviations used are: BioID, proximity-based biotinylation; CHX, cyclohexamide; EDMD, Emery-Dreifuss Muscular Dystrophy.

(Fig. 1*A*). Since interactors are covalently modified with biotin, robust lysis conditions can be used to solubilize polypeptides localized to poorly soluble cellular compartments (10, 12–16). Moreover, since this method does not require that protein-protein interactions be maintained post-lysis, weak and/or transient interactors may also be identified. We reasoned that BioID may be exploited to capture ubiquitin E3 ligase substrates and tested this notion here.

The human beta transducin repeat-containing polypeptides β-TrCP1 (*FBXW1*) and β-TrCP2 (*FBXW11*) are evolutionarily conserved paralogous F-box proteins sharing >80% amino acid sequence identity and >90% homology, and act as substrate recognition components of SCF (Skp1-Cullin-F-box) complexes (17). A number of β-TrCP substrates have been well documented, implicating these ligases in numerous biological functions, including regulation of the NFκB, Hippo, Wnt and Hedgehog signaling pathways (18–21). Some β-TrCP targets harbor the sequence DSGX(n)S or variants thereof. Phosphorylation of this sequence is required for SCF$^{\beta\text{-TrCP1/2}}$ binding and thus regulates the half-life of these "phosphodegron"-containing proteins (21, 22). However, other *bona fide* SCF$^{\beta\text{-TrCP1/2}}$ substrates contain highly degenerate or non-canonical degrons, which are thought to mediate constitutive turnover (21). A single, simple linear sequence motif that could predict β-TrCP binding has thus not been defined.

Here we demonstrate that BioID performed on cells treated with the proteasome inhibitor MG132 can recover many of the previously characterized substrates and stable interactors of β-TrCP1/2. Using semi-quantitative mass spectrometry, we identify and validate a number of new substrates, linking these well-studied E3 ligases to several new biological functions. The method used here is simple, scalable, and should be broadly applicable for the identification of substrates for many other E3s.

EXPERIMENTAL PROCEDURES

Cloning—All PCR reactions were performed using Q5 DNA polymerase (NEB) according to manufacturer's instructions. Primers, destination plasmids, cloning sites and DNA templates are listed in supplemental Table S4. PCR products were digested with AscI and NotI (NEB) and ligated into the destination plasmid using T4 DNA ligase (NEB) following manufacturer's instructions. The PPP1R15B S459–466A phosphodegron mutant was generated by PCR-driven overlap extension (23) using WT PPP1R15B external primers and the overlapping internal primers listed in supplemental Table S4.

BioID—BioID (10) was carried out essentially as we described previously (12). In brief, full length human β-TrCP1 (BC027994) and β-TrCP2 (BC026213) coding sequences were amplified by PCR and cloned into our pcDNA5 FRT/TO FLAGBirA* expression vector (see primers in supplemental Table S4). Using the Flp-In system (Invitrogen), 293 T-REx Flp-In cells stably expressing FLAGBirA*-β-TrCP1 or FLAGBirA*-β-TrCP2 were generated. After selection (DMEM + 10% FBS + 200 μg/ml Hygromycin B), 10 × 150 cm^2 plates of subconfluent (60%) cells were incubated for 24 h in complete media supplemented with 1 μg/ml tetracycline (Sigma) and 50 μM biotin (BioShop, Burlington, ON, Canada). Five plates were treated with 5 μM MG132 (calpain inhibitor IV, Z-Leu-Leu-Leu-CHO; American Peptide Company, Sunnyvale, CA). Cells were collected and pelleted (2000 rpm, 3 min), the pellet was washed twice with PBS, and dried pellets were snap frozen. Pellets were lysed in 10 ml of modified RIPA lysis buffer (50 mM Tris-HCl pH 7.5, 150 mM NaCl, 1 mM EDTA, 1 mM EGTA, 1% Triton X-100, 0.1% SDS, 1:500 protease inhibitor mixture (Sigma-Aldrich, Saint-Louis, MO), 250U Turbonuclease (Accelagen, San Diego, CA)) at 4°C for 1 h, then sonicated (30 s at 35% power, Sonic Dismembrator 500; Fisher Scientific) to disrupt visible aggregates. The lysate was centrifuged at 16000 rpm (35000 × *g*) for 30 min. Clarified supernatants were incubated with 30 μl packed, pre-equilibrated streptavidin-Sepharose beads (GE) at 4 °C for 3 h. Beads were collected by centrifugation (2000 rpm, 2 min), washed six times with 50 mM ammonium bicarbonate pH 8.3, and treated with TPCK-trypsin (Promega, Madison, WI, 16 h at 37 °C). The supernatant containing the tryptic peptides was collected and lyophilized. Peptides were resuspended in 0.1% formic acid and 1/6th of the sample was analyzed per MS run.

FLAG Affinity Purification—For FLAG pulldowns, 10 × 150 cm^2 dishes of FLAGBirA*-β-TrCP1 or FLAGBirA*-β-TrCP2 293 T-REx cells were treated with tetracycline and biotin as above (5 plates were treated with 5 μM MG132), scraped into PBS, pooled, washed twice in 25 ml PBS and collected by centrifugation at 1000 × *g* for 5 min at 4 °C. Cell pellets were stored at −80 °C until lysis. The cell pellet was weighed and 1:4 pellet weight/lysis buffer (by volume) was added. Lysis buffer consisted of 50 mM HEPES-NaOH (pH 8.0), 100 mM KCl, 2 mM EDTA, 0.1% Nonidet P-40, 10% glycerol, 1 mM PMSF, 1 mM DTT and 1:500 protease inhibitor mixture (Sigma-Aldrich, St. Louis, MO). Upon resuspension, cells were incubated on ice for 10 min, subjected to one additional freeze-thaw cycle, then centrifuged at 27000 × *g* for 20 min at 4 °C. Supernatant was transferred to a fresh 15 ml conical tube and 250U Turbonuclease (Accelagen) plus 30 μl packed, pre-equilibrated FLAG-M2 agarose beads (Sigma-Aldrich) were added. The mixture was incubated for 2 h at 4 °C with end-over-end rotation. Beads were pelleted by centrifugation at 1000 rpm (100 × *g*) for 1 min and transferred with 1 ml of lysis buffer to a fresh centrifuge tube. Beads were washed once with 1 ml lysis buffer and twice with 1 ml ammonium bicarbonate (ammbic) rinsing buffer (50 mM ammbic pH 8.0, 75 mM KCl). Elution was performed by incubating the beads with 150 μl of 125 mM ammonium hydroxide (pH >11). The elution step was repeated twice more, and the combined eluate centrifuged at 15000 × *g* for 10 min, transferred to a fresh centrifuge tube and lyophilized. Following overnight trypsin digestion (as above), peptides were resuspended in 0.1% formic acid and 1/6th of the sample was analyzed per MS run.

Mass Spectrometry—Liquid chromatography (LC) analytical columns (75 μm inner diameter) and precolumns (150 μm ID) were made in-house from fused silica capillary tubing from InnovaQuartz (Phoenix, AZ) and packed with 100Å C_{18}-coated silica particles (Magic, Michrom Bioresources, Auburn, CA). LC-MS/MS was conducted using a 120 min reversed-phase buffer gradient running at 250 nl/min (column heated to 40 °C) on a Proxeon EASY-nLC pump in-line with a hybrid LTQ-Orbitrap velos mass spectrometer (Thermo Fisher Scientific). A parent ion scan was performed in the Orbitrap, using a resolving power of 60000. Simultaneously, up to the twenty most intense peaks were selected for MS/MS (minimum ion count of 1000 for activation) using standard CID fragmentation. Fragment ions were detected in the LTQ. Dynamic exclusion was activated such that MS/MS of the same *m/z* (within a 10 ppm window, exclusion list size 500) detected three times within 45 s were excluded from analysis for 30 s. For protein identification, .raw files were converted to the .mzXML format using Proteowizard (24), then searched using X!Tandem (25) against Human RefSeq Version 45 (containing 36113 entries). Search parameters specified a parent MS tolerance of 15 ppm

and an MS/MS fragment ion tolerance of 0.4 Da, with up to two missed cleavages allowed for trypsin. Oxidation of methionine was allowed as a variable modification. Data were analyzed using the trans-proteomic pipeline (26) via the ProHits 2.0.0 software suite (27). Proteins identified with a ProteinProphet cut-off of 0.85 (corresponding to ≤1% FDR) were analyzed with SAINT Express v. 3.3 (28, 29). For BioID, 24 control runs were used for comparative purposes; eight runs of a BioID analysis conducted on cells expressing the FlagBirA* tag only, eight runs of BioID conducted on untransfected 293 T-REx cells, and eight runs from a BioID analysis conducted on an unrelated bait protein. In each case, four runs were conducted on untreated cells and four runs were conducted on cells treated with MG132, as above. The 24 controls were collapsed to the highest four spectral counts for each hit. Similarly, for Flag IP-MS analysis, 24 control runs were conducted; FLAG IP-MS analyses of three unrelated FLAGBirA*-tagged proteins expressed in 293 T-REx cells, in the presence and absence of MG132. The 24 control runs were collapsed to the highest four spectral counts for each hit. All data are publically available and have been uploaded to the MassIVE archive (massive.ucsd.edu) ID: MSV000079032. Annotated spectra are available for inspection via the MS-Viewer tool (30) of Protein Prospector (prospector2.ucsf.edu; see supplemental Table S1 for all associated file keys).

Interactor Classification—Based on four independent MS runs (two technical replicates and two biological replicates for each bait, in the presence and absence of MG132), *bona fide* interactors were defined as high confidence protein identifications (ProteinProphet *p* value >0.85) displaying a SAINT score ≥0.75. Histones were removed manually. Fold-change was calculated as: $\log_2$ (1+ spectral count sum in the presence of MG132)/(1+ spectral count sum in the absence of MG132). Statistical significance of the difference between the spectral counts detected in samples prepared from cells cultured with and without MG132 was calculated using Student's *t* test. Hits considered as putative substrates display a $\log_2$ fold change ≥ 1 (Table I) and *p* value ≤ 0.05. Gene ontology (GO) category assignments detailed in supplemental Table S3.

Substrate Validation, Cycloheximide (CHX) Chase, and Immunoblotting—At day 0, 5 × 10^5 293 T-REx Flp-In cells were transfected with 20 nM siRNA Control (siCONTROL non-targeting siRNA #1 Thermo Scientific); 10 nM siRNA β-TrCP1: *CGGAAGAGUUUUUCGACUAtt* (predesigned Invitrogen ID:s17110) + 10 nM siRNA β-TrCP2: *GGUUGUUAGUGGAUCAUCAtt* (predesigned Invitrogen ID:s23485); or 20 nM siRNA β-TrCP1/2: *GUGGAAUUUGUGGAACAUCtt* (31) using Lipofectamine RNAiMAX (Invitrogen), according to manufacturer's instructions. On day one, transfection media was removed and replaced by fresh media, and cells were subjected to a second transfection with epitope-tagged (3xHA, FLAG or FLAGBirA*) substrate candidates in pcDNA3 or pcDNA5 using PolyJet transfection reagent (Signagen, Rockville, MD) according to manufacturer's instructions. On day 2, cells were trypsinized and 10^5 cells/well were distributed to a 24-well plate. On day 3, CHX (100 μg/ml) was added for 0–8 h. Upon collection, media was removed and 80 μl of 95 °C SDS lysis buffer (50 mM TrisHCl pH 6.8, 2% SDS, 20% glycerol, 50 mM DTT, bromphenol blue) was added to each well. Cells in lysis buffer were scraped and transferred to an Eppendorf tube, incubated 5 min at 95 °C, and briefly sonicated. Twenty microliters of each sample was loaded on a 4–12% Criterion™ XT Bis-Tris Gel (Bio-Rad, Hercules, MD). Proteins were transferred to nitrocellulose (BioTrace NT (Pall, Mississauga, ON, Canada) CA27376–991) and blocked 1 h in PBS 0.01% Tween + 5% skim milk or 5% BSA. Antibodies were diluted in blocking agent and used as follows: HA.11 Clone 16B2 (Covance, Princeton, NJ) 1:5000 16 h 4 °C; FLAG M2 (Sigma) 1:2000 16 h 4 °C; anti-β-actin (C4; Santa-Cruz, Dallas, TX) 1:2000 16 h 4 °C; mAb414 (Covance) 1:5000 16 h 4 °C, Streptactin-HRP 1:5000 1 h RT. Membranes were washed with PBS 0.01% Tween, and incubated 1 h in PBS 0.01% Tween with 1:10000 Goat anti-Mouse IgG (H + L)-HRP Conjugate (BioRad #1706516). Membranes were washed four times with PBS 0.01% Tween and revealed using Clarity Western ECL substrate (Bio-Rad, Hercules, MD) enhanced chemiluminescence reagent.

Western Blot Quantification—Band intensities were quantified using ImageJ software, using arbitrary pixel intensity units. Each 3xHA or FLAG signal was normalized to the corresponding anti-β-actin signal for the same lane. Each lane is then presented as a fraction of the band intensity at time zero for that treatment.

Immunofluorescence, Image Acquisition, and Processing—Untransfected HeLa cells or HeLa stable cell lines expressing FLAG-SUN2 were grown on poly-L-Lysine (Sigma) coated coverslips, fixed with 4% formaldehyde for 15 min, and washed in PBS with 0.1% Triton X-100. Cells were blocked in 5% BSA in PBS for 30 min before incubating in PBS with 1:1000 anti-FLAG M2 (Sigma), anti-Lamin B (Abcam) or anti-SUN2 (Sigma) primary antibodies for 1h at RT. Anti-mouse Alexa 488 and Streptavidin-Alexa594 (Life Technologies) were used at 1:1000 and 1:5000, respectively, and incubated at RT for 1 h. After removing the solution, cells were incubated with 1 μg/ml of 4′,6-diamidino-2-phenylindole (DAPI) in PBS for 5 min. After washing with PBS 3 × 5 min, coverslips were mounted with ProLong Gold Antifade (Thermo Fischer Scientific). Cells were imaged using a Plan-Apo 60X oil lens, NA 1.40 on an Olympus FV1000 confocal microscope (zoom factor between 3 and 5; Olympus America, Melville, NY). Images were processed using the Volocity Viewer v.6 and assembled using Adobe Illustrator CS5 (Adobe System Inc., San Jose, CA).

Live Cell Imaging, P-body and Stress Granule Quantification—GFP and mCherry constructs were generated by Gateway cloning into an N- or C-terminal pDEST pcDNA5/FRT/TO-eGFP, or an N-terminal pDEST pcDNA5/FRT/TO-mCherry vector. Clone accession numbers are shown in supplemental Table S4. Stable Flp-In HeLa T-REx cell line pools were generated as described in (32). The PATL1, DCP1A, EIF4A1, PABPC1 and G3BP1 genes were cloned from the following clone accession number templates: AM392959, DQ893260, DQ893044, DQ893508, and DQ893058. For live-cell studies, cultured HeLa cells transiently transfected with pcDNA3 Cherry-SUN2 or stably transfected with the GFP or mCherry-tagged P-body or stress granule markers were transfected with siRNA control or siRNA β-TrCP1/2 in 24-well plates, incubated 48 h, then seeded into Lab-Tek chambers (Thermo Fisher) and treated for 24 h with 1 μg/ml tetracycline to induce marker expression. HeLa cells were imaged without additional treatment. P-body and stress granule marker expressing cells were stained with 1 μg/ml of Hoechst 33342 dye (Fisher Scientific) for 15 min at 37 °C. Cells were washed twice with warm PBS before incubating 45 min in phenol red-free complete media with 500 μg/ml arsenite (Sigma Aldrich). Cells were incubated in a Chamlide TC stage incubator (LCI, Seoul, Korea) during acquisition (37 °C; 5% CO_2). The Volocity 6 measurement tool was used to calculate the number of P-bodies or stress granules per cell. Size and brightness parameters were adjusted specifically for each bait protein to delineate the relevant structures, and identical acquisition and calculation parameters were applied under all conditions for a given fluorescent marker (*i.e.* fixed exposure time, sensitivity and gain, and constant size and intensity thresholds for nuclei, P-bodies and stress granules). Volocity 6 software was used to generate the stitched composite image from 4 × 4 adjacent fields acquired with 10% overlap at 60× magnification, or 3 × 3 adjacent fields acquired with 10% overlap at 20X magnification. Four stacks (500 nm *z* axis distance spread) were acquired for each field. Nuclei were defined as Hoechst/DAPI positive objects with a minimal volume of 150 μm^3 (to avoid counting micronuclei). All cells were seeded at a comparable density (to reach 80% at analysis time) and ≥100 cells were acquired per condition. Five independent experiments were conducted for P-body quantitation,

and six independent experiments were conducted for stress granules. Cells treated with siRNA control or siRNA β-TrCP1/2 were compared and statistical significance assessed using Student's *t* test. supplemental Figs. S3*B* and S4 display the stitched field, extended focus images used for the analysis, and indicate a homogeneous distribution of P-bodies and stress granules among siRNA control and siRNA β-TrCP1/2-treated cells.

Flag Co-IP—FLAGBirA*-β-TrCP1 or FLAGBirA*-β-TrCP2 293 T-REx cells were transfected at 50–70% confluence with either pcDNA3 3xHA-PPP1R15B wt or pcDNA3 3xHA-PPP1R15B S459–466A using the Polyjet reagent, following manufacturer's instructions. 16 h post-transfection, each 10 cm plate was split 1:4, cells were treated with 1 μg/ml tetracycline for 24 h and 10 μM MG132 for 2 h prior to harvesting. Each plate was washed once with PBS, then cells were scraped and re-suspended in 5 ml PBS with 2 mM EDTA. Cells were pelleted at 2000 rpm for 2 min, resuspended in 1 ml PBS, and transferred to an Eppendorf tube, pelleted again at 2000 rpm for 2 min, PBS was removed, and the cell pellet was snap frozen. Cell pellets were lysed in 1 ml TAP lysis buffer (50 mM Hepes-NaOH pH 8, 150 mM NaCl, 10% glycerol, 2 mM EDTA, 0.1% IGEPAL, 2 mM DTT, 1:500 protease inhibitor (Sigma), 10 mM NaF, 0.25 mM sodium orthovanadate, 50 mM β-glycerol phosphate) for 1 h on an end-over-end rotator at 4 °C, and centrifuged at 20000 rpm for 15 min at 4 °C. Five percent of the cleared lysates was set aside to serve as input, and the remaining lysate was incubated with 20 μl packed anti-FLAG M2 Affinity Gel beads (Sigma Aldrich A2220) on an end-over-end rotator overnight at 4 °C. Beads were pelleted at 2000 rpm for 2 min and washed 5 times with TAP lysis buffer before adding 60 μl boiling Laemmli buffer. Samples were boiled and spun at 15000 rpm to pellet beads prior to loading supernatant onto SDS gel.

In Vivo Ubiquitylation Assay (Denaturing Lysis, Nondenaturing IP)—293 T-REx cells stably expressing FLAG-PPP1R15B WT or FLAG-PPP1R15B S459–466A were transfected at 50–70% confluence with pcDNA3 3xHA-ubiquitin using PolyJet reagent, as per manufacturer's instructions. 16 h post-transfection, each 10 cm^2 plate was split to treat for the following conditions: (1) no tetracycline (tet) +MG132, (2) +tet -MG132, (3) +tet +MG132 (1 μg/ml tetracycline 24 h, 10 μM MG132, 2 h). Each 10 cm^2 plate was washed once with PBS and cells were resuspended in 5 ml PBS with 2 mM EDTA. Cells were pelleted at 2000 rpm for 2 min, resuspended in 1 ml of PBS and transferred to an Eppendorf tube. 50 μl of resuspended cells were set aside for "input". These were pelleted again at 2000 rpm for 2 min and snap frozen. Cells pellets were lysed in 500 μl denaturing lysis buffer (1% SDS, 50 mM Tris-HCl pH 6.8, 10 mM DTT, 1:500 protease inhibitor (Sigma)), sonicated 3 × 10 s and centrifuged at 20,000 rpm for 15 min at 4 °C. Cleared lysates were diluted with 4.5 ml PBS + 0.1% Nonidet P-40 and incubated with 20 μl packed anti-FLAG M2 Affinity Gel beads on an end-over-end rotator overnight at 4 °C. Beads were pelleted at 2000 rpm for 2 min and washed 5× with PBS + 0.1% Nonidet P-40, before adding 80 μl boiling Laemmli buffer. Samples were boiled and centrifuged at 2000 rpm to pellet beads, prior to loading supernatant onto SDS gel.

ER Stress Response Assay—293 T-REx Flp-In cells stably expressing FLAG-PPP1R15B WT or FLAG-PPP1R15B S459–466A were seeded into a six well plate. Cultures were treated with tetracycline (1 μg/ml), along with thapsigargin (1 μM) or tunicamycin (1 μg/ml) for 24 h. Cells were collected, washed in 1x PBS and lysed in 100 μl TAP lysis buffer (see above; *n.b.* wash and lysis buffers also contained the ER stress drugs at the same concentrations used in culture). Cell lysates were centrifuged at 20,000 rpm for 15 min at 4 °C. Supernatant was removed and protein content quantified for normalization. Phospho-eIF2α (Ser51) and eIF2α antibodies (Cell Signaling Technology, Beverly, MA) were used at 1:1000 dilution in TBST.

Cell Viability Assay—293 T-REx Flp-In cells stably expressing FLAG-PPP1R15B WT or FLAG-PPP1R15B S459–466A were seeded into a 96-well plate at a density of 4000 cells per well. Tetracycline (1 μg/ml, 72 h) was added to the cultures for 24 h to induce protein expression, then cells were treated with the indicated concentration of tunicamycin (48 h). Each condition was performed in triplicate. To assess viability, 20 μl of 1 μg/ml MTT (Sigma) dissolved in sterile PBS was added to 100 μl of media in each well and incubated for 2 h at 37 °C until purple precipitate was visible. 120 μl of Stop Reagent (0.04N HCl and 10% Triton-X 100 in isopropanol) was added to each well and the media resuspended to dissolve the precipitate. Plates were read at 570 nm and 630 nm; OD_{570} - OD_{630} values for each well were determined and the triplicate measurement was averaged for each condition. Each average value was normalized to the untreated sample of the corresponding cell line, and standard error calculated. This experiment was repeated three times, with a representative experiment displayed in Fig. 4*F*.

RESULTS

BioID Identifies Known and Novel SCF$^{\beta\text{-TrCP1/2}}$ Substrates—SCF$^{\beta\text{-TrCP1}}$ and SCF$^{\beta\text{-TrCP2}}$ target substrates for 26S proteasome-mediated degradation. We reasoned that, using the BioID method, stable β-TrCP1/2 interacting partners (such as other components of the SCF complex) should be labeled with biotin to a similar extent in the presence and absence of MG132, whereas substrates should be stabilized when proteasome activity is impaired, resulting in increased abundance in the streptavidin pulldown. A simple semiquantitative mass spectrometry approach could then be employed to identify these putative substrates.

Previous reports have indicated that N-terminally tagged β-TrCP maintains proper function (22, 33–36), and our own preliminary BioID analysis indicated that N-terminal FLAG-BirA*-tagged β-TrCP1 recovered more stable interactors (*e.g.* SCF complex components) and previously reported substrates than a C-terminally tagged protein (data not shown). A FLAGBirA* tag was thus fused to the N terminus of β-TrCP1 and 2 (to generate FLAGBirA*-β-TrCP1 and FLAGBirA*-β-TrCP2), and these proteins were stably expressed in 293 T-REx Flp-In cells. Two independent stable cell pools were created for each bait protein. The FLAGBirA*-β-TrCP polypeptides were expressed in a tetracycline-regulated manner, and biotinylated protein species were detected by Western analysis following the addition of biotin to the culture media (Fig. 1*B*). Cells were lysed using a modified RIPA buffer (see Experimental procedures), followed by sonication and nuclease treatment to maximize the solubilization of proteins localized to poorly soluble intracellular locations, or associated with membranes, RNA or chromatin. Biotin-labeled proteins were captured using a streptavidin-Sepharose matrix. After washing, streptavidin-bound proteins were treated with trypsin, and the eluted peptides identified using nanoflow liquid chromatography-electrospray ionization-tandem mass spectrometry (nLC-ESI-MS/MS). Untransfected cells, cell pools expressing the FLAGBirA* tag alone, and cells expressing an unrelated bait protein were subjected to the same analysis to control for endogenously biotinylated proteins and

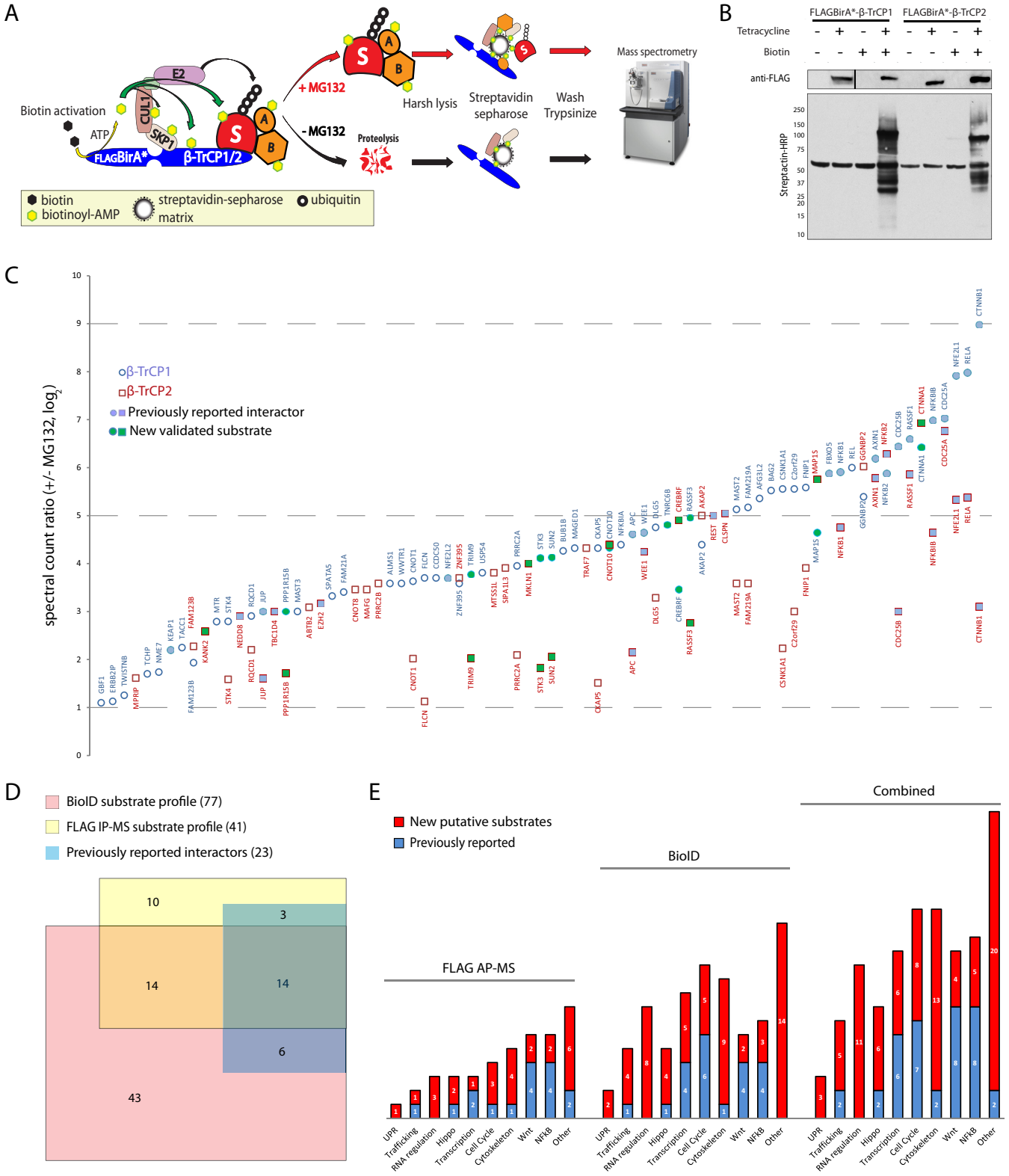

FIG. 1. **BioID can be used to identify ubiquitin E3 ligase substrates.** *A*, An N-terminal tag consisting of the FLAG epitope and the mutant *E. coli* biotin conjugating protein BirA R118G (BirA*) was fused to the N terminus of the human F-box proteins β-TrCP1 and β-TrCP2. The BirA* protein converts biotin (*black* hexagon) to biotinoyl-AMP (*yellow* hexagon). The mutant BirA protein exhibits a reduced affinity for the activated biotin molecule; biotinoyl-AMP thus diffuses away and reacts with free amine groups on lysine residues in nearby polypeptides, including *e.g.* the bait protein itself, other SCF complex components (CUL1, SKP1), SCF substrates (S) and substrate binding partners (A, B). In the presence

polypeptides that interact nonspecifically with the streptavidin or solid phase support.

Using the ProHits (27) system, MS data were analyzed with the X!Tandem database search algorithm (25), and the resulting peptide identifications subjected to ProteinProphet (37) analysis. Finally, the data were subjected to Significance Analysis of INTeractomes (SAINT) (28, 29) to identify *bona fide* SCF$^{\beta\text{-TrCP1/2}}$ interacting partners. Polypeptides identified with a ProteinProphet confidence value ≥0.85 and assigned a SAINT score ≥0.75 are listed in supplemental Table S1.

Two hundred ninety two unique polypeptides were identified as high confidence SCF$^{\beta\text{-TrCP1/2}}$ interactors using this technique (supplemental Table S1). As expected, this list includes known components of the SCF complex and a number of previously reported substrates (supplemental Table S2). Notably, in the presence of MG132, 20 previously characterized SCF$^{\beta\text{-TrCP1/2}}$ substrates (beta-catenin (*CTNNB1*), CDC25A, CDC25B, claspin (*CLSPN*), NRF2 (*NFE2L2*), junction plakoglobin (JUP), RASSF1, REST, TAZ (*WWTR1*), WEE1, *etc.*) were identified with +MG132/untreated spectral count ratios ≥2. In contrast, the known stable SCF$^{\beta\text{-TrCP1/2}}$ components SKP1, CUL1, RBX1, CDC34 (*UBE2R1*), UBE2R2, USP47 and NRD1 were detected with +MG132/untreated spectral count ratios < 2, as expected for proteins that are not stabilized in response to proteasome inhibition (supplemental Table S1). The fold-change in spectral counts in response to MG132 treatment was highly reproducible between biological replicates of the same bait protein (R^2 = 0.88 and 0.85 for β-TrCP1 and β-TrCP2, respectively; supplemental Figs. S1*A*, S1*B*).

Using this information, we categorized the previously unreported SCF$^{\beta\text{-TrCP1/2}}$ interactors as substrate candidates if the +MG132/untreated spectral count ratio was ≥2 ($\log_2 > 1$). Applying these parameters, 77 polypeptides displayed a "substrate profile" in the FLAGBirA*-β-TrCP1 and/or FLAG-BirA*-β-TrCP2 BioID analyses (Fig. 1*C* and Table I).

To determine how the BioID method compares to a standard IP approach, a standard FLAG tag-based immunopurification (FLAG IP-MS; see Experimental procedures) was also conducted on FLAGBirA*-β-TrCP1/2 (as above, in the presence and absence of MG132) and the associated proteins identified using MS/MS. In this case, 127 high confidence β-TrCP1/2 interactors were identified (Fig. 1*D* and supplemental Table S1). 41 proteins displayed a substrate profile, 28 of which (~70%) were identified with a similar profile in BioID (Fig. 1*D* and Table I). 17 previously reported substrates and substrate interacting partners were identified with this method. Thirteen additional proteins with a substrate profile were detected that were not also identified in BioID (Fig. 1*D*, Table I and supplemental Table S1). Together, these data suggested that BioID could represent a valuable complement to standard IP-based approaches for the identification of E3 targets.

Consistent with previous reports, many of the proteins displaying a substrate profile in both the BioID and FLAG IP-MS data sets are involved in cell cycle regulation, Wnt, NFκB, and Hippo signaling (Fig. 1*E*). Notably, however, several specific functional categories - all of which are associated with less soluble cellular compartments and not previously linked with β-TrCP function - were enriched in the BioID data set, including *e.g.*; cytoskeleton, vesicle trafficking and RNA regulation (FLAG: 5, 2, 3 *versus* BioID: 10, 5, and 8 identified polypeptides, respectively; Fig. 1*E*).

BioID Identifies β-TrCP Substrate Candidates—To begin to characterize the new putative SCF$^{\beta\text{-TrCP}}$ substrates, a number of candidates (selected to represent a variety of different biological functions, and localized to different intracellular compartments) were expressed as epitope (FLAGBirA*, FLAG or 3xHA)-tagged proteins in 293 T-REx cells. Cultures were treated with cycloheximide (CHX) to inhibit protein synthesis, and protein half-lives were monitored in the presence of: (1) a single siRNA targeting both β-TrCP1 and β-TrCP2 (31); (2) a combination of two siRNAs, each directed against a single β-TrCP paralog, and; (3) a scrambled control siRNA. Although the control siRNA had no effect, the siRNAs directed against the β-TrCP1/2 transcripts efficiently reduced FLAGBirA*-β-TrCP1/2 protein expression levels (Fig. 2*A*). β-TrCP1/2 knockdown had no apparent effect on β-actin expression levels (Fig. 2*A*) or the FG repeat-containing nuclear pore complex proteins recognized by mAb414 (38) (Fig. 2*B*). However, as

of the 26S proteasome inhibitor MG132, β-TrCP substrates are stabilized. Following cell lysis under stringent buffer conditions, biotinylated proteins are affinity purified using streptavidin coupled to Sepharose beads. Streptavidin-bound proteins are washed and subjected to trypsin proteolysis, and the liberated peptides are identified using tandem mass spectrometry. *B*, Expression of FLAGBirA*-β-TrCP1/2 leads to biotinylation of endogenous proteins. 293 T-REx cells expressing FLAGBirA*-β-TrCP1 or FLAGBirA*-β-TrCP2 were treated with tetracycline (1 μg/ml) to induce protein expression, and with biotin (50 μM) to enable proximity-dependent polypeptide labeling. Whole cell lysates were subjected to SDS-PAGE and immunoblotted with an anti-FLAG antibody (*top* panel) or streptavidin-HRP (horseradish peroxidase; *bottom* panel). *C*, β-TrCP1/2 interactors displaying a substrate profile. Proteins identified in the BioID analysis with a ProteinProphet score ≥0.85 (corresponding to ≤1% FDR), a SAINT score ≥0.75, and a spectral count ratio (+MG132/untreated) $\log_2 > 1$. *Circles*, polypeptides identified in β-TrCP1 BioID; *squares*, proteins identified in β-TrCP2 BioID. Previously identified β-TrCP interactors are highlighted in *blue*. Proteins demonstrated in this study to be stabilized following β-TrCP1/2 knockdown (see Fig. 2 and Supplemental Fig. 2) are highlighted in *green*. *D*, Overlap of FLAG IP-MS and BioID substrate candidates. Diagram highlighting the overlap between BioID hits displaying a substrate profile (*pink*), FLAG IP-MS hits displaying a substrate profile (*yellow*), and previously reported β-TrCP interactors (*blue*). *E*, Functional categories of FLAG IP-MS and BioID substrate candidates. Numbers of previously reported β-TrCP interactors within each category are indicated in *blue* and numbers of new substrate candidates in each category indicated in *red*.

TABLE I

β-TrCP BioID and FLAG IP-MS hits displaying a "substrate profile." FLAGBirA-β-TrCP1 and FLAGBirA*-β-TrCP2 BioID and FLAG IP-MS results. Data are presented as spectral counts detected for each prey protein, as indicated. Two technical replicates were performed on each of two unique biological replicates for each bait protein (for a total of four MS analyses), in both the presence and absence of MG132 (5uM, 24 hrs). ProteinProphet confidence score p ≥ 0.85, SAINT score ≥0.75. For control runs, only the highest four spectral counts (out of 24 runs) are shown. *log_2 ratio of total spectral counts detected for each of the indicated polypeptides in the presence vs. the absence of MG132. One spectral count was added to all totals for this analysis, to avoid division by 0. All ratios shown were statistically significant ($p < 0.05$) as determined by student's t-test (blank values not significant and/or not identified as a high confidence interactor with the corresponding technique and bait protein). β-TrCP1 substrate candidates indicated in light blue, β-TrCP2 substrate candidates indicated in green. Previously reported β-TrCP1/2 interactor gene names are highlighted in bold. Proteins demonstrated here to be stabilized following β-TrCP knockdown (Fig. 2 and supplementary Fig. S2) are boxed in dark blue, with white font*

	BioID												IP-MS											
	β-TrCP1							β-TrCP2						β-TrCP1						β-TrCP2				
Gene Name (Alias)	Controls	- MG132	Total	+ MG132	Total	+/-MG132 (log2)*		- MG132	Total	+ MG132	Total	+/-MG132 (log2)*	Controls	- MG132	Total	+ MG132	Total	+/-MG132 (log2)*		- MG132	Total	+ MG132	Total	+/-MG132 (log2)*
CTNNB1				136 136 117 115	504	8.98		15 19 16 16	66	145 150 137 142	574	3.10		23 25 3	51	232 192 187 197	808	3.96		2 4 1 2	9	313 286 342 279	1220	6.93
RELA				61 52 72 67	252	7.98		1	1	27 16 16 23	82	5.38				47 38 35 37	157	7.30				10 9 6 6	31	5.00
NFE2L1 (NRF1)	9 8 7 5			59 53 68 60	240	7.91		2 1 1	4	56 54 37 53	200	5.33				16 13 14 13	56	5.83						
CDC25A				24 24 38 43	129	7.02				29 23 28 28	108	6.77		12 10	22	41 40 43 35	159	2.80				33 27 27 22	109	6.78
NFKBIB (IKBB)				31 29 37 29	126	6.99				8 5 5 6	24	4.64				31 26 17 15	89	6.49				2	2	
RASSF1				22 19 28 27	96	6.60				19 13 9 16	57	5.86				15 15	30					7 10 8 10	35	5.17
CDC25B				21 26 22 17	86	6.44		2 2 2	6	14 16 11 14	55	3.00		23 22 9 12	66	54 50 28 24	156	1.23	2	1 1	4	8 8 9 6	31	2.68
CTNNA1				22 28 17 18	85	6.43				36 25 22 38	121	6.93		5	5	138 109 38 40	325	5.76				86 95 107 63	351	8.46
AXIN1				26 15 13 18	72	6.19				12 18 11 13	54	5.78				40 43 33 23	139	7.13				14 5 14 13	46	5.55
REL				7 12 22 22	63	6.00										5 7 4	16	4.09						
NFKB1				15 14 18 12	59	5.91				10 3 7 6	26	4.75				42 34 13 13	102	6.69						
NFKB2				18 16 11 13	58	5.88				24 14 12 27	77	6.29				46 40 14 18	118	6.89				13 13 15 4	45	5.52
FBXO5				18 13 13 14	58	5.88																		
FNIP1				11 16 9 11	47	5.58		1	1	8 6 13 2	29	3.91												
C2orf29 (CNOT11)				15 11 10 10	46	5.55				2 3 2	7	3.00												
CSNK1A1	6			13 12 11 10	46	5.55	5	4	9	16 11 10 9	46	2.23	1			14 10 10 9	43	5.46				2	2	
BAG2	6 5 2			14 12 14 5	45	5.52	3 5 2 5		15	7 2 1 3	13													
GGNBP2				11 15 10 5	41	5.39				18 18 13 15	64	6.02				10 7	17					7 4 4 1	16	4.09
AFG3L2 (SCA28)				12 8 11 9	40	5.36																		
FAM219A				8 7 11 9	35	5.17				3 3 5	11	3.58												
MAST2				9 9 9 7	34	5.13				3 2 4 2	11	3.58												
RASSF3				7 9 4 10	30	4.95	2	2	4	7 11 9 6	33	2.77												
TNRC6B	3			5 10 8 4	27	4.81																		
DLG5				8 10 2 6	26	4.75		2 1	3	15 10 5 8	38	3.29												
MAP1S				6 6 8 4	24	4.64				18 12 10 13	53	5.75		1	1	5	5					3 3 4 3	13	3.81
WEE1				7 4 6 7	24	4.64				7 4 2 5	18	4.25												
APC		8 5 6	19	130 134 113 109	486	4.61	32 39 39 32		142	204 155 125 151	635	2.15		40 29	69	168 159 140 136	603	3.11	8 8 12		28	105 115 146 80	446	3.95
NFKBIA (IKBA)				4 6 4 6	20	4.39				3	3					6 6 5	17	4.17						
AKAP2				6 6 5 3	20	4.39																		
CNOT10	1	2 3 1	6	36 38 34 32	140	4.33		1	1	14 10 8 9	41	4.39												
CKAP5	33 26 24 23	2 5 3 3	13	75 72 70 62	279	4.32	26 28 22 26		102	94 80 43 76	293	1.51												
MAGED1				4 6 4 5	19	4.32				1 3 2	6													
BUB1B	5 4 3 2	3 1	4	24 30 24 17	95	4.26				1	1													
SUN2		1 5 5 3	14	64 63 67 67	261	4.13	14 11 10 9		44	58 47 38 43	186	2.06		19 7 6 5	37	50 41 7 10	108	1.52	1	1 3	5	16 11 10 4	41	2.81
STK3 (MST2)	1	3 7 2	12	57 53 59 55	224	4.11	10 10 10 10		40	45 34 28 37	144	1.82		9 5	14	35 31 7 12	85	2.52	2 1 3 6		12	13 18 17 6	54	2.08
PRRC2A	16 11 8 8	2 4 4	10	47 42 39 41	169	3.95	15 5 10 6		36	64 31 28 34	157	2.09												
USP54				3 3 4 3	13	3.81	1		1															
TRIM9	2 1	4 3 1 1	9	29 35 43 29	136	3.78	2 4 4 3		13	14 17 11 14	56	2.03				41 32 23 21	117	6.88				16 13 18 5	52	5.73
FLCN				6 3 3	12	3.70	1 1 4 4		10	6 8 3 6	23	1.13												
CCDC50				2 2 3 5	12	3.70				2 2 1	5													
NFE2L2 (NRF2)				3 1 3 5	12	3.70				8	8													
CNOT1	9 7 6 4	3 2 3 1	9	37 36 26 24	123	3.63	18 16 15 12		61	91 52 42 65	250	2.02		6 7	13	34 22 1	57			2 1	3	2 5 4 1	12	1.70
ZNF395				3 3 3 2	11	3.58				6 3 3	12	3.70				6 6	12					4 2 2	8	3.17
ALMS1				3 3 2 3	11	3.58																		
WWTR1 (TAZ)				3 2 3 3	11	3.58				2	2													

expected, the known SCF$^{\beta\text{-TrCP}}$ substrate NFE2L2 (NRF2; Fig. 2*C*, *top*) (39) was efficiently stabilized in response to β-TrCP1/2 knockdown (apparent half-lives indicated below each blot). Of the 13 substrate candidates assayed here, 12 were efficiently stabilized following β-TrCP knockdown: SUN2, TRIM9, CREBRF, CTNNA1, CNOT10, TNRC6B (Fig. 2*D*), KANK2, STK3 (MST2), MAP1S, MKLN1, RASSF3 (supplemental Fig. S2*A*) and PPP1R15B (Fig. 3). In contrast, the FNIP1 protein displayed a substrate profile, but did not appear to be stabilized in response to β-TrCP knockdown (supplemental Fig. S2*B*). As discussed below, this protein is therefore likely to be a substrate interacting partner rather than a direct β-TrCP substrate.

Together, these findings demonstrate that BioID can be used as an effective complement to standard IP-MS or other techniques for the identification of Ub E3-associated proteins. Indeed, in this experimental setting, BioID not only provided confirmatory data for the majority of FLAG IP-MS hits display-

TABLE I—*continued*

CREBRF (LRF)				2 3 3 2	10	3.46			8 11 4 6	29	4.91											
FAM21A	7	2 1 1	4	10 16 12 14	52	3.41	9 7	16	18	18												
SPATA5				3 4 2	9	3.32																
PPP1R15B (CREP)		3 4 3	10	20 27 19 21	87	3.00	6 5 8 5	24	21 19 22 19	81	1.71				17 11 6 6	40	5.36			5 4 6 4	19	4.32
JUP	1	2 2	4	14 14 11	39	3.00	8 8 7	23	18 16 21 17	72	1.60											
MAST3				3 2 2	7	3.00			1 4	5												
RQCD1		1	1	3 4 4 3	14	2.91	1 1 2	4	5 10 4 3	22	2.20											
STK4 (MST1)	1	9 5	14	24 29 23 27	103	2.79	7 8 8 8	31	29 29 14 23	95	1.58				24 25 5 7	61	5.95			13 17 16 5	51	5.70
MTR	2	1 5 5	11	21 23 20 18	82	2.79			4 1 2	7												
KEAP1	5	7 12 8 9	36	44 42 42 41	169	2.20	3 3 6 2	14	5 8 2 9	24												
FAM123B (WTX)		2 3 3 2	10	10 12 10 9	41	1.93	6 5	11	15 17 10 15	57	2.27		5 5	10	18 22 7 5	52	2.27			3 4 5	12	3.70
NME7		2	2	2 2 3 2	9	1.74																
TCHP		1 1 1	3	3 4 3 2	12	1.70			3 1 4	8												
TWISTNB		2 4 2 4	12	9 7 8 6	30	1.25	1 2 5	8	2 2 2 2	8												
ERBB2IP	4 4 3 2	7 7 7 5	26	12 21 12 13	58	1.13	6 2 5 6	19	7 4 3 7	21												
GBF1 (ARF1GEF)		8 18 18 12	56	42 41 19 19	121	1.10	48 47 46 46	187	69 44 33 56	202					47 30 8 8	93	6.55			19 18 19 14	70	6.15
CLSPN	7 5 4 2			10 10 4 4	28		1	1	25 19 6 15	65	5.04											
REST									10 9 4 8	31	5.00				2	2				6 7 12	25	4.70
TRAF7									6 5 2 6	19	4.32											
MKLN1 (TWA2)									4 3 5 3	15	4.00											
SIPA1L3				3 1 1	5				4 5 1 4	14	3.91											
MTSS1L				4 1 1	6				5 5 1 2	13	3.81											
PRRC2B	10 6 5 5			20 18 9 11	58		5 3 3	11	33 35 44 31	143	3.58											
CNOT8									4 2 4	10	3.46											
MAFG									2 2 2 4	10	3.46											
EZH2									2 2 4	8	3.17											
ABTB2							1	1	5 2 4 5	16	3.09											
TBC1D4				1 4 5	10		1	1	7 2 2 4	15	3.00											
NEDD8		12 11 5 7	35	20 20 17 13	70		3	3	5 9 15	29	2.91									5 5 6	16	4.09
KANK2 (SIP)	2	3 2 4 5	14	9 6 6 5	26		1 1	2	4 4 4 5	17	2.58											
TACC1	3 2			2 3	5		3 1 3	7	10 14 3 10	37	2.25											
MPRIP		1	1	1 3	4		2 3 3 8	16	15 17 7 12	51	1.61											
HCFC1															18 10 7 5	40	5.36					
HSPB1															5 1 3 5	14	3.91					
CUL1		160 163 155 157	635	225 241 230 210	906		123 114 123 108	468	209 200 152 180	741			39 31 27 32	129	97 94 71 71	333	1.36	10 8 9 8	35	147 144 169 115	575	4.00
YWHAG													33 26 25	84	49 44 50 46	189	1.16	14	14	34 29 39 31	133	3.16
CTNNA2															26	26				27 31 46 20	124	6.97
UBAP2L												3 2 1			5 4 1 1	11				9 11 10 2	32	5.04
CSTF2T												2								5 7 9	21	4.46
TFAP4		10 14 11 14	49	5 3 9 7	24		15 13 12 13	53	19 16 9 8	52					1 1	2				4 5 7 3	19	4.32
PDCD4	1 1 1	17 27 25 20	89	24 21 42 31	118		35 30 32 23	120	23 21 10 13	67			42 38 46 39	165	23 18 28 30	99		1	1	5 5 7 3	20	3.39
IRS2													7 4	11	6 3	9		1	1	5 2 6 2	15	3.00
YWHAB													46 39 40 37	162	66 58 80 75	279		25 26 23 27	101	87 87 93 54	321	1.66
YWHAZ												5 4	38 38 29 25	130	58 53 51 48	210		18 18 13 13	62	50 43 56 35	184	1.55
YWHAE												19 14 14 12	74 58 60 57	249	124 109 125 124	482		60 65 59 62	246	156 162 168 113	599	1.28

ing a substrate profile (Table I, Fig. 1*D*), but also identified many additional substrate candidates (Fig. 1*D* and 1*E*).

BioID Identifies E3 Substrates in the Context of Protein Complexes—β-catenin (*CTNNB1*) is a well-characterized β-TrCP substrate (22, 33–35) identified with high confidence in our analysis (Table I, Fig. 1*D*). In the absence of Wnt signaling, β-catenin is bound and phosphorylated by the β-catenin destruction complex (19). The newly created β-TrCP phosphodegron recruits SCF$^{\beta\text{-TrCP}}$, which effects its ubiquitylation. Surprisingly, multiple β-catenin destruction complex components (APC, AXIN1, CSNK1A1, and FAM123B) also displayed a substrate profile in our BioID data set, even though these proteins are not direct SCF$^{\beta\text{-TrCP}}$ targets (Fig. 1*C*, Table I). However, these findings are consistent with a recent report demonstrating that β-catenin is targeted by SCF$^{\beta\text{-TrCP}}$ within the context of an intact destruction complex (40): since BioID is a proximity-based labeling method, when β-catenin is stabilized by MG132 treatment we may thus expect to observe increased biotinylation of both β-catenin and components of the destruction complex. It is therefore important to note that stabilizing a substrate (*via* MG132 treatment) that is part of a larger protein complex can lead to increased biotinylation of both the direct substrate and its interacting partners. This information can add significant value regarding the context in which a given substrate is targeted, but additional analysis of the complex will sometimes be required to identify the direct substrate(s) contained therein.

β-TrCP-dependent Degradation of SUN2 is Critical for Nuclear Membrane Integrity—The LINC (linker of nucleoskeleton and cytoskeleton) complex is composed of SUN (Sad1/UNC-84) proteins localized to the inner nuclear membrane, and KASH (Klarischt/ANC-1/SYNE homology) domain-containing polypeptides localized to the outer nuclear membrane. SUN proteins interact with nuclear lamina components, and KASH domain-containing polypeptides interact with cytoplasmic cytoskeletal proteins. Together, the SUN and KASH proteins are critical for the maintenance of proper nuclear morphology and anchorage (41).

3xHA-SUN2 was dramatically stabilized (with an apparent >4-fold increase in half-life and a >2.5-fold increase in steady-state protein levels) by β-TrCP1/2 knockdown (Fig. 2*D*). Notably, knockdown of SCF$^{\beta\text{-TrCP1/2}}$ was also associated with defects in nuclear morphology: while the control siRNA had no effect, 27% of cells treated with the β-TrCP1/2 siRNA

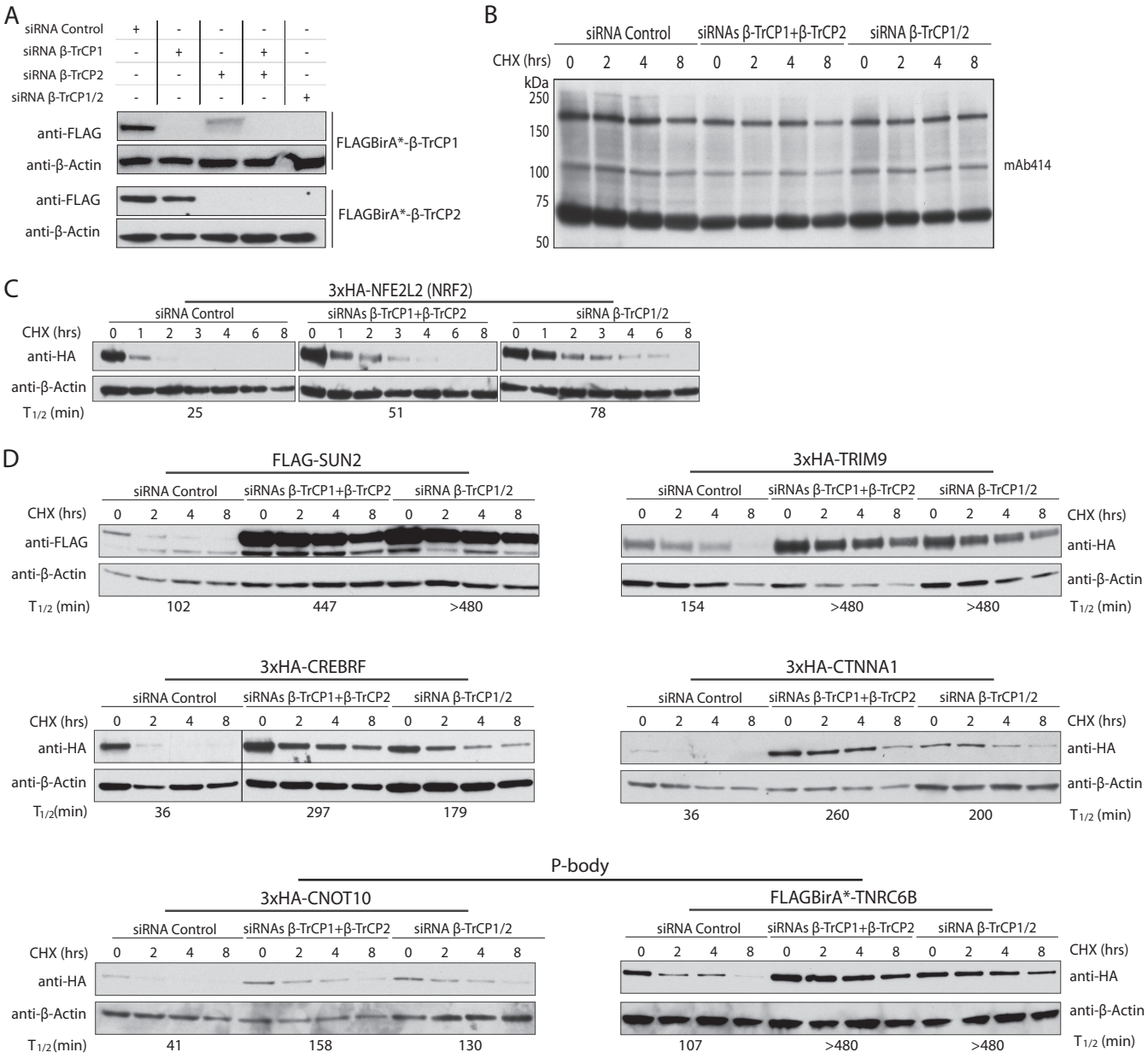

FIG. 2. **Validation of new β-TrCP substrates detected with BioID.** *A*, Validation of β-TrCP siRNAs. Lysates from 293 T-REx cells expressing FLAGBirA*-β-TrCP1 or FLAGBirA*-β-TrCP2 in the presence of: (i) a control siRNA; (ii) two siRNAs, each directed against an individual β-TrCP paralog, or; (iii) a single siRNA directed against both β-TrCP1 and β-TrCP2 (β-TrCP1/2) were subjected to anti-FLAG Western analysis, as indicated. Actin blots are loading controls. *B*, Depletion of β-TrCP does not affect the half-lives of nuclear pore complex FG proteins. 293 T-REx cells were transfected with control or the indicated β-TrCP siRNAs, and treated with cycloheximide (CHX) for the indicated times. Whole cell lysates from these cells were subjected to 4–12% SDS-PAGE, and Western analysis conducted using mAb414, which recognizes FG repeat-containing nuclear pore complex proteins. *C*, 293 T-REx cells expressing 3xHA-NFE2L2 were transfected with control or β-TrCP siRNAs, as indicated, then treated with CHX for the indicated times. Whole cell lysates were subjected to 4–12% SDS-PAGE, then probed for NFE2L2 protein expression using an anti-HA antibody. The apparent half-life ($T_{½}$) of 3xHA-NFE2L2 is indicated below each blot. *D*, Validation of novel β-TrCP substrate candidates. 293 T-REx cells expressing the indicated epitope-tagged proteins were transfected with control or β-TrCP siRNAs (as indicated) and treated with CHX for the indicated times. Protein expression levels were characterized using HA or FLAG antibodies. Apparent protein half-lives (in minutes) are indicated below each blot.

displayed misshapen nuclei accompanied by nuclear membrane blebbing, as detected using antisera directed against endogenous SUN2 (Fig. 3*A*), FLAG-SUN2 (expressed stably in HeLa T-REx cells) and endogenous Lamin B (Fig. 3*B*, supplemental Fig. S3*A*). Consistent with these observations, over-expression of mCherry-SUN2 (via transient transfection) was also associated with widespread nuclear membrane blebbing and morphological defects, and this effect was ex-

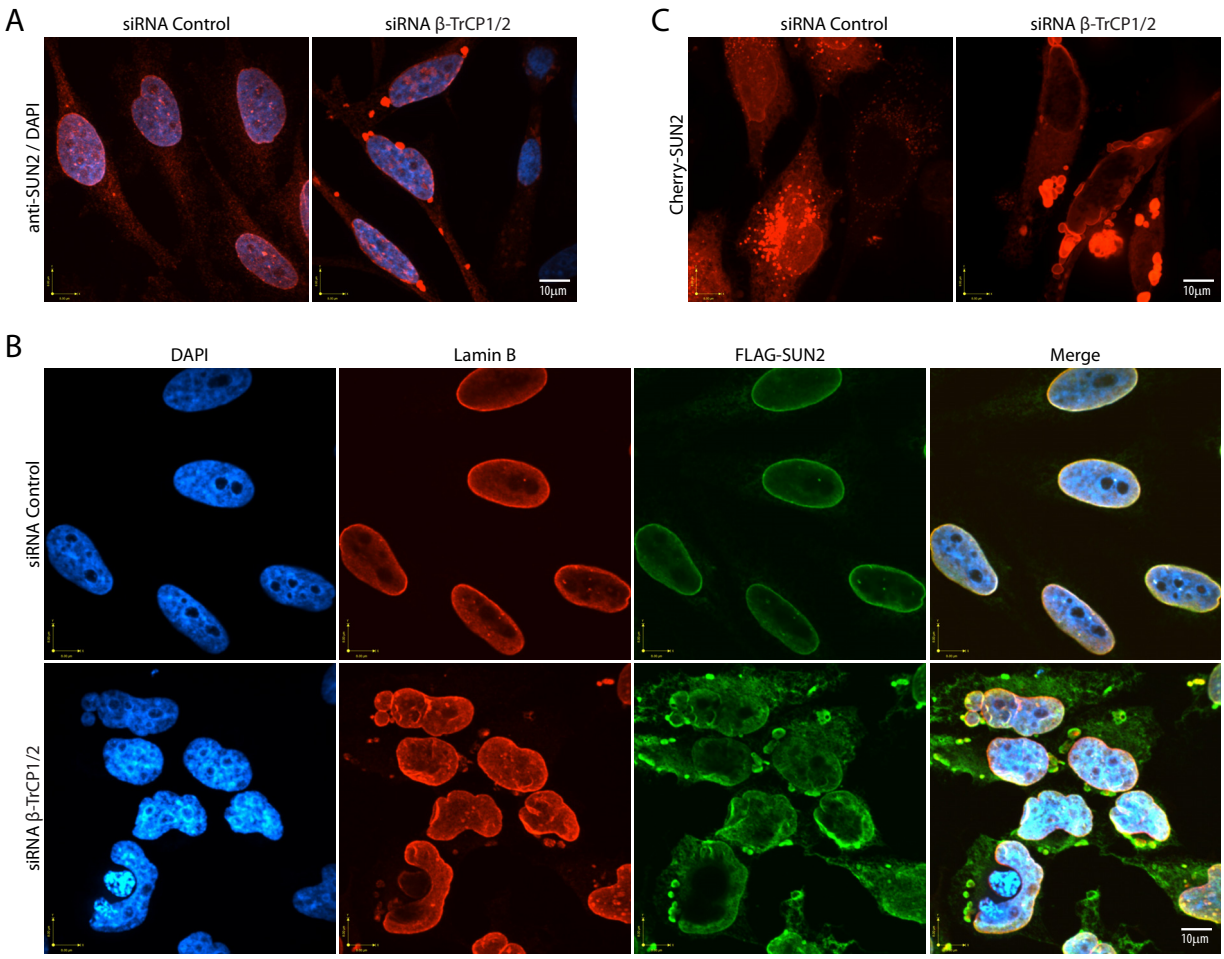

FIG. 3. **Stabilization of SUN2 by β-TrCP affects nuclear membrane structure.** *A*, HeLa cells were treated with control or β-TrCP1/2 siRNA, and immunofluorescence (IF) microscopy was conducted using antibodies directed against endogenous SUN2 (*red*). DNA stained with DAPI (*blue*). *B*, IF of HeLa cells expressing FLAG-SUN2 and transfected with the indicated siRNA: anti-FLAG (*green*); anti-Lamin B (*red*); DAPI (*blue*). *C*, Live cell imaging of HeLa cells transiently transfected with mCherry-SUN2 and control or β-TrCP1/2 siRNA.

acerbated by knockdown of β-TrCP1/2 (Fig. 3C; supplemental Movie S1). Together, these data suggest that SCF$^{\beta\text{-TrCP}}$ plays an important role in the maintenance of nuclear membrane structure, and reveal a direct link between the control of SUN2 expression levels and the maintenance of nuclear membrane integrity. While further study will be required to understand the precise relationship between SUN2 levels and nuclear membrane structure, the defects associated with SUN2 misexpression are similar to phenotypes previously reported in fibroblasts derived from Emery-Dreifuss Muscular Dystrophy (EDMD) patients bearing mutations in LINC complex-associated nuclear lamina components such as *LMNA* and *STA* (42).

β-TrCP function is Linked to P-body Abundance—Interestingly, many of the new β-TrCP1/2 targets identified by BioID are involved in mRNA turnover, silencing and translational control. For example, CNOT1, CNOT8, RQCD1 (CNOT9), CNOT10 and C2ORF29 (CNOT11) are all components of the CCR4-NOT complex, which catalyzes the removal of mRNA poly(A) tails prior to mRNA decay (43) and plays an important role in RNA-mediated gene silencing, along with an additional putative target identified here - TNRC6B (a GW182 protein) (44). All of these proteins localize to processing (P)-bodies, poorly soluble, dynamically regulated cytoplasmic ribonucleoprotein particles enriched in translation factors and mRNA decay proteins (45).

To begin to explore the role of SCF$^{\beta\text{-TRCP1/2}}$ in the regulation of mRNP particles, P-bodies were visualized in live cells expressing GFP- or mCherry-tagged forms of the P-body markers DCP1A (Fig. 4A and supplemental Fig. S4*A*) or PATL1 (supplemental Fig. S4*A*). Previous studies have demonstrated that overexpression or depletion of P-body components can affect P-body number (46). Consistent with our observation that CCR4-NOT components and TNRC6B are stabilized in response to β-TrCP knockdown (Fig. 2*D*), P-body number was significantly increased in cells treated with siRNA directed against β-TrCP1/2 (3.46 ± 0.37 P-bodies/cell), as compared with cells treated with the scrambled siRNA control (1.49 ± 0.02 P-bodies/cell; $n = 5$ experiments, $p < 0.001$; Fig.

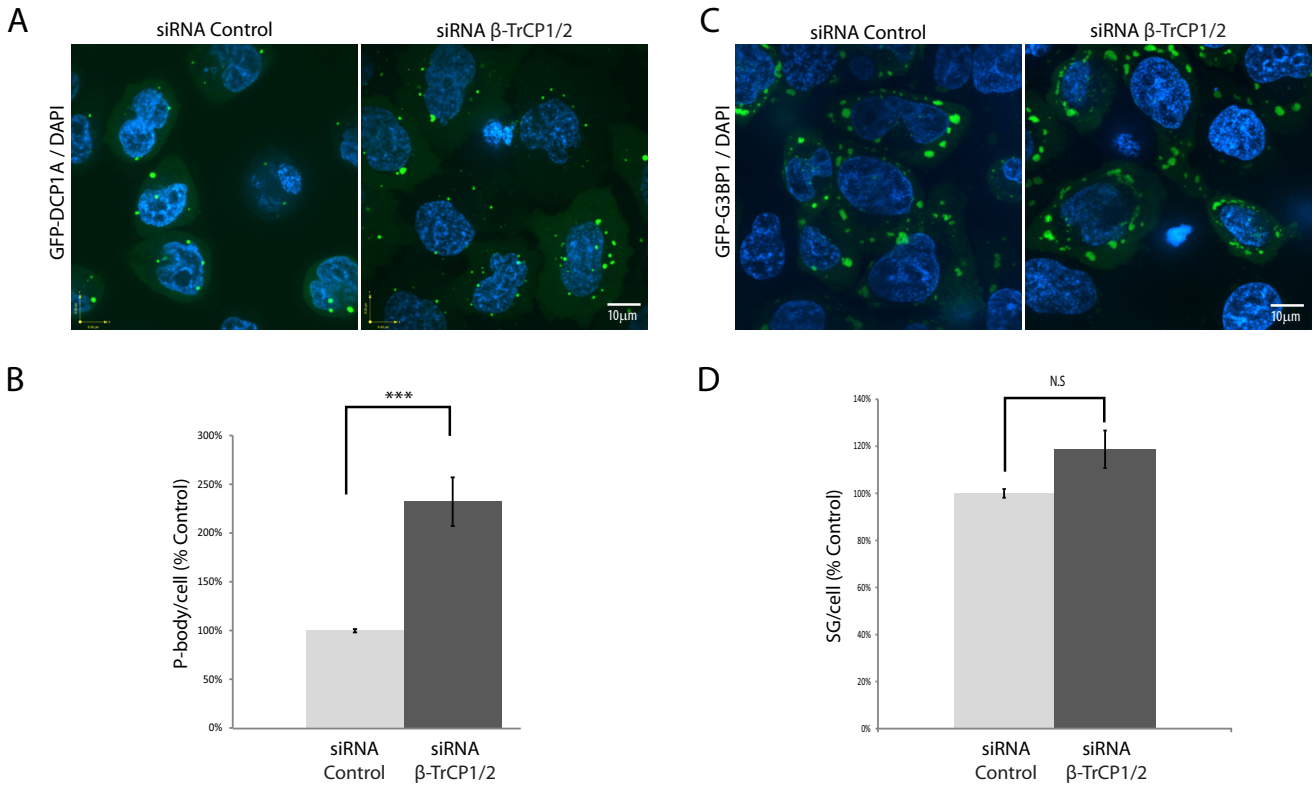

	siRNA Control (20nM)					
	expt1 GFP-DCP1A	expt2 Cherry-DCP1A	expt3 GFP-DCP1A	expt1 GFP-PATL1	expt2 GFP-PATL1	Average +/- SE
# cells	112	106	198	122	759	
# P-bodies	175	149	297	183	1107	
P-body/cell (avg)	**1.56**	**1.41**	**1.50**	**1.50**	**1.46**	**1.49 +/- 0.02**
	siRNA β-TrCP1/2 (20nM)					
	expt1 GFP-DCP1A	expt2 Cherry-DCP1A	expt3 GFP-DCP1A	expt1 GFP-PATL1	expt2 GFP-PATL1	
# cells	170	87	241	162	610	
# P-bodies	491	390	913	384	2295	
P-body/cell (avg)	**2.89**	**4.48**	**3.79**	**2.37**	**3.76**	**3.46 +/- 0.37**

	siRNA Control (20nM)						
	expt1 GFP-PAPBC1	expt2 GFP-PAPBC1	expt1 GFP-G3BP1	expt2 GFP-G3BP1	expt1 GFP-EIF4A1	expt2 GFP-EIF4A1	Average +/- SE
# cells	119	143	127	169	134	158	
# stress granules	384	457	425	525	476	508	
Stress granules/cell (avg)	**3.23**	**3.20**	**3.35**	**3.11**	**3.55**	**3.22**	**3.27 +/- 0.06**
	siRNA β-TrCP1/2 (20nM)						
	expt1 GFP-PAPBC1	expt2 GFP-PAPBC1	expt1 GFP-G3BP1	expt2 GFP-G3BP1	expt1 GFP-EIF4A1	expt2 GFP-EIF4A1	
# cells	120	134	105	138	144	196	
# stress granules	563	643	433	455	495	584	
Stress granules/cell (avg)	**4.69**	**4.80**	**4.12**	**3.30**	**3.44**	**2.98**	**3.89 +/- 0.31**

FIG. 4. **β-TrCP modulates P-body formation.** *A*, HeLa Flp-In T-REx cells expressing the P-body marker GFP-DCP1A were transfected with control or β-TrCP1/2 siRNA and treated with tetracycline (1 μg/ml, 24 h) and arsenite (500 μM, 45 min), as indicated. *B*, Live cell confocal microscopy was conducted and P-body number quantified using Volocity software (see Experimental procedures). *C*, HeLa Flp-In T-REx cells expressing the stress granule marker GFP-G3BP1 were transfected with control or β-TrCP1/2 siRNA and treated with tetracycline and arsenite, as above. *D*, Live cell confocal microscopy was conducted and stress granule number quantified, as above. N.S.; not significant.

4*B*, supplemental Fig. S4*A*). This did not appear to be a general effect on RNA metabolism, as knockdown of β-TrCP1/2 had little or no impact on the number of stress granules (SG), another type of cytoplasmic mRNP particle (as measured here with the SG markers G3BP1, PABPC1, and eIF4A1; Fig. 4*C*–4*D*, supplemental Fig. S4*B*). While further study will be required to understand its precise role in the regulation of mRNA metabolism, these data implicate β-TrCP in P-body function.

β-TrCP Targets PPP1R15B to Regulate eIF2α Phosphorylation—PPP1R15B (also known as CReP; constitutive reverter of eIF2α phosphorylation) (47) is a regulatory subunit of the Ser/Thr protein phosphatase 1 (PP1). In this capacity, PPP1R15B targets PP1 to the eukaryotic translation initiation factor 2 alpha (eIF2α) protein. eIF2α is phosphorylated on Ser51 (by multiple kinases) in response to *e.g.* protein folding stress and viral infection (48). eIF2α phosphorylation levels regulate the rate at which the translation initiation factor eIF2 can form a complex with charged initiator methionyl-tRNA and deliver it to the 40S ribosomal subunit to initiate protein synthesis (48). Increased eIF2α Ser51 phosphorylation attenuates translation initiation to curb protein synthesis rates. Under basal conditions, PPP1R15B constitutively targets PP1 to eIF2α to maintain low levels of phosphorylated Ser51 (47). Proper regulation of eIF2α phosphorylation is critical for the maintenance of cellular homeostasis, as *e.g.* mice lacking the *Ppp1r15b* gene display severe growth retardation, hematopoietic system dysfunction and early embryonic lethality (49), and cells lacking PPP1R15B display a defective environmental stress response (47).

FLAG-PPP1R15B half-life was dramatically increased (from 20–30 min to >70 min) following β-TrCP depletion, resulting

in a >1.7-fold increase in steady-state expression levels (Fig. 5*A*). Notably, PPP1R15B contains a putative phosphodegron (SDSSLSDS, aa 459–466) that could be recognized by SCF$^{\beta\text{-TrCP1/2}}$ (22). The five serine residues in this region were thus mutated to alanines (S459–466A) and the half-life of the resultant mutant protein characterized. Similar to that observed in response to β-TrCP knockdown, PPP1R15B S459–466A displayed a substantially longer half-life than the wild type (WT) polypeptide (Fig. 5*B*). In addition, even though it is expressed at higher steady-state levels, the HA-PPP1R15B S459–466A mutant protein was co-immunoprecipitated with FLAG-β-TrCP1/2 much less efficiently than the WT protein (Fig. 5C), directly linking the integrity of the phosphodegron to β-TrCP binding.

Cells co-expressing WT or S459–466A FLAG-PPP1R15B with HA-ubiquitin were next lysed under denaturing conditions (see Experimental procedures), the lysate was diluted and FLAG-tagged PPP1R15B proteins isolated by immunoprecipitation. As expected (because of increased steady-state expression levels), increased quantities of the mutant PPP1R15B were immunoprecipitated (see anti-FLAG blot, Fig. 5*D*, *bottom panel*). However, anti-HA Western blotting revealed considerably lower ubiquitylation levels of this protein, as compared with its WT counterpart (Fig. 5*D*, *top panel*). Together, these data strongly suggest that PPP1R15B is a β-TrCP substrate and that Ser459–466 represents a *bona fide* β-TrCP phosphodegron.

eIF2α pSer51 phosphorylation levels in cells expressing WT or S459–466A PPP1R15B proteins were next monitored in the presence and absence of tunicamycin or thapsigargin, compounds that elicit ER stress by interfering with protein glycosylation or depletion of ER calcium stores, respectively. As expected, eIF2α Ser51 phosphorylation was increased in cells expressing the WT PPP1R15B protein in response to ER stress (Fig. 5*E*). In cells expressing the PPP1R15B S459-S466A mutant protein, eIF2α phosphorylation was also increased, but to a much lesser extent (Fig. 5*E*). The proper regulation of steady-state PPP1R15B protein levels is thus critical for the proper regulation of eIF2α phosphorylation in response to protein folding stress. Finally, similar to that previously observed in eIF2α Ser51Ala mouse embryo fibroblasts (50), expression of the PPP1R15B S459–466A mutant protein sensitized cells to ER stress, as measured by cell viability in the presence of increasing doses of tunicamycin (Fig. 5F). Together, our data validate PPP1R15B as an SCF$^{\beta\text{-TrCP}}$ substrate, and reveal an important role for this E3 ligase in the regulation of translation initiation.

DISCUSSION

Understanding the targeting landscape of the ubiquitin system represents a major challenge in cell biology. The identification of E3 ligase substrates has been difficult, in part because: (1) ligase - substrate interactions are often of very low-affinity (generally in the high nM to microMolar (μM) range) and/or transient in nature; (2) many substrates are subjected to rapid proteasomal degradation, and therefore cannot be detected using standard techniques; (3) the human ubiquitome is extremely complex, and therefore difficult to study and; (4) many substrate proteins are localized to poorly soluble cellular compartments, making their isolation and identification by standard IP-based techniques problematic.

Here we demonstrate that BioID combined with semi-quantitative mass spectrometry, conducted on cells in the presence and absence of MG132, can be used for the identification of E3 substrates. Focusing on the well-studied F-box proteins β-TrCP1 and β-TrCP2, we identified a number of established targets along with numerous new substrate candidates, implicating β-TrCP in several novel biological functions.

An important limitation of IP-based approaches for the characterization of protein-protein interactions is that no particular buffer combination and cell lysis procedure can be expected to both maintain all protein-protein interactions (and especially weak or transient E3-substrate interactions) and simultaneously solubilize all proteins in a cell. Since BioID utilizes a covalent biotin modification to mark bait protein interactors, the maintenance of protein-protein interactions is not required for their identification, and harsh lysis techniques may be used to liberate proteins from poorly soluble cellular fractions that are often not accessed by IP-compatible buffers. The straightforward, scalable technique presented here is thus highly complementary to standard IP-MS approaches, and is likely to be broadly applicable for E3 substrate identification.

A Role for β-TrCP in the Maintenance of the Nuclear Membrane—As a component of the LINC complex, the new β-TrCP substrate SUN2 plays an important role in the maintenance of nuclear integrity, intracellular nuclear positioning and nuclear membrane structure (51). Mutations in LINC complex components (and LINC complex interacting partners) have been associated with EDMD, a progressive muscular dystrophy characterized by myofiber degeneration and cardiomyopathy. EDMD muscle biopsies and primary fibroblasts derived from EDMD patients display frequent abnormal nuclear lobulation and herniation, accompanied by the presence of micronuclei (52–54). These reports are consistent with our observations in cells with misregulated SUN2 levels.

Although the *SUN1* and *SUN2* genes have not yet been directly linked to EDMD, these LINC proteins clearly represent promising candidates for further study. (Indeed, the currently defined gene mutations associated with EDMD have been found in less than half of EDMD patients (51)). Although additional study will also be required to better understand the role of β-TrCP in the regulation of nuclear membrane structure and function, our data reveal a critical link between this E3 ligase and control of a LINC complex component.

A Role for β-TrCP in the Cellular Stress Response—β-TrCP is the E3 ligase for IκB, which sequesters the NFκB complex

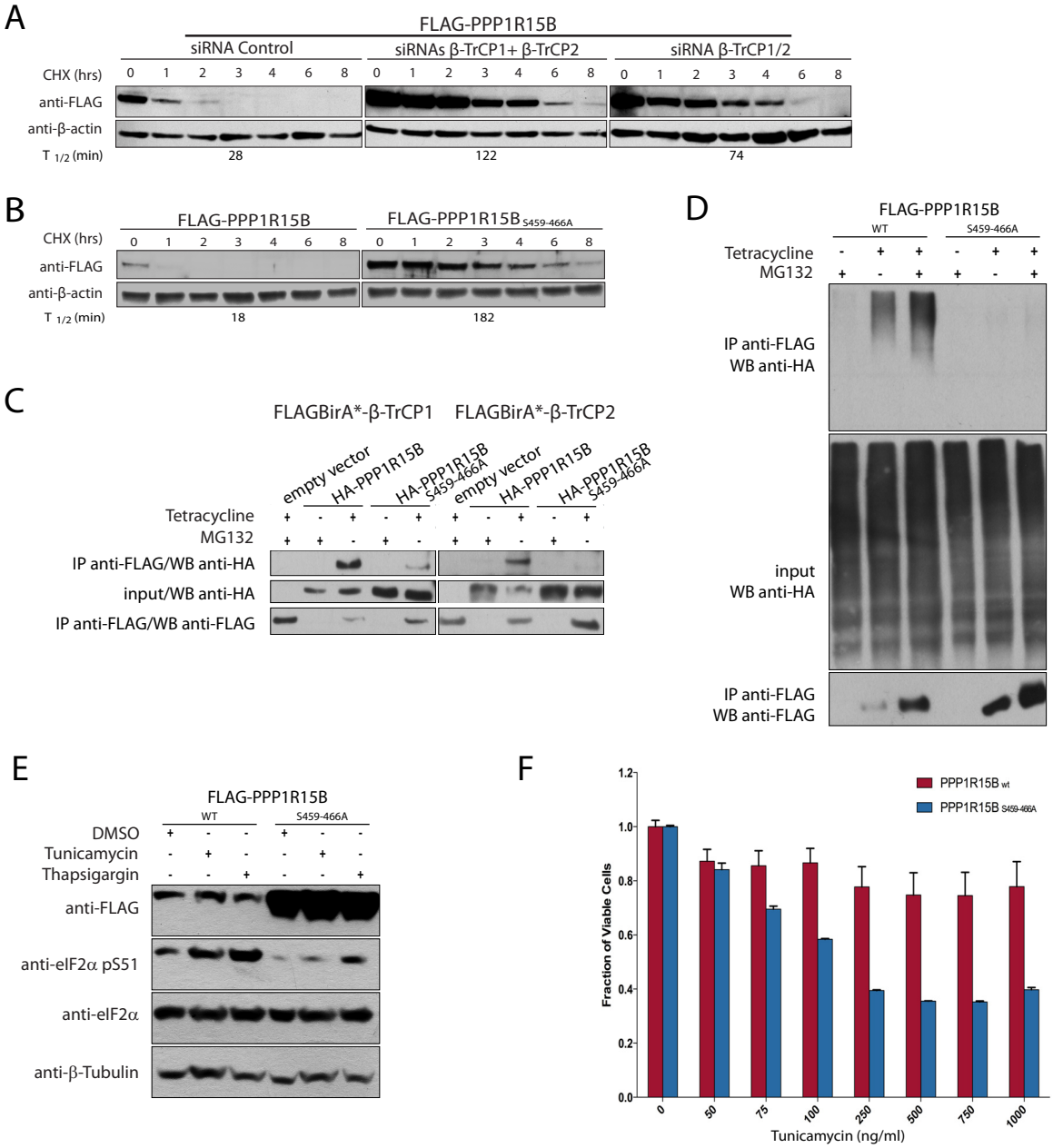

FIG. 5. **FLAG-PPP1R15B is stabilized by β-TrCP knockdown.** *A*, Western blot analysis of lysates derived from 293 T-REx cells expressing FLAG-PPP1R15B treated with control or β-TrCP siRNA, as indicated. *B*, A PPP1R15B phosphodegron mutant is stabilized. 293 T-REx cells expressing FLAG-tagged WT or the S459–466A PPP1R15B phosphodegron mutant were treated with CHX for the indicated times. Cell lysates were subjected to Western blotting with antibodies directed against FLAG and beta actin. Apparent half lives of the FLAG-tagged PPP1R15B proteins are indicated below each blot. *C*, The β-TrCP interaction is disrupted in a PPP1R15B phosphodegron mutant. Co-immunoprecipitation of FLAGBirA*-β-TrCP1/2 with HA-tagged WT or S459–466A PPP1R15B proteins. *D*, Mutation of the phosphodegron disrupts PPP1R15B ubiquitylation. 293 T-REx cells were co-transfected with plasmids coding for FLAG-PPP1R15B WT or S459–466A and HA-ubiquitin. Lysates were prepared under denaturing conditions, diluted and FLAG IPs conducted. The isolated proteins were subjected to Western blot analysis with anti-FLAG and anti-HA. Whole cell lysates were probed with anti-HA. *E*, Expression of the PPP1R15B phosphodegron mutant results in decreased eIF2α Ser51 phosphorylation levels. Cell lsyates derived from 293 T-REx cells expressing FLAG-tagged WT or S459–466A PPP1R15B phosphodegron mutant proteins, and treated with vehicle (DMSO) or the ER stress agents tunicamycin or thapsigargin, were subjected to Western blotting, as indicated. *F*, Expression of the PPP1R15B phosphodegron mutant imparts sensitivity to ER stress agents. 293 T-REx cells expressing WT or phosphodegron mutant PPP1R15B proteins were exposed to the indicated concentrations of tunicamycin for 24 h. Viable cells, as detected by MTT assay (untreated culture numbers set to 1) are displayed ($n = 3$; a representative experiment is shown).

in the cytoplasm. When IκB is phosphorylated by the IκB kinase (IKK) in response to *e.g.* viral infection, tissue damage or other types of cellular stress, the newly created phosphodegron recruits SCF$^{\beta\text{-TrCP}}$. Once IκB is degraded, the NFκB complex can translocate to the nucleus to effect stress-adaptive changes in the transcription program.

Our data reveal previously unidentified links between β-TrCP and other proteins involved in the cellular stress response. P-bodies play important roles in the regulation of RNA stability, and P-body formation and turnover is highly regulated in response to cellular stress (45, 55). eIF2α phosphorylation levels are also regulated in response to many types of stress, including *e.g.* viral infection, protein folding stress and nutrient deprivation (48). β-TrCP may therefore represent an important hub for modulating the proteome in response to cellular stress: *i.e.* in addition to effecting changes in the transcriptome via NFκB activation, the regulation of translation via the sequestration or degradation of pre-existing mRNAs in P-bodies, combined with a global reduction in translation initiation rates via increased eIF2α phosphorylation levels, could represent a rapid and efficient way to re-program the entire proteome in response to stress. Further study will be focused on understanding the role of SCF$^{\beta\text{-TrCP}}$ in the cellular stress response.

BioID as a Complementary Approach for the Identification of E3 Substrates—While our work was in progress, two additional studies were published on the identification of β-TrCP substrates (56, 57), utilizing more standard IP-MS and TAP (tandem affinity purification)-MS approaches. Notably, despite the use of widely disparate approaches, many of the same β-TrCP interactors were detected among all three studies, significantly expanding the number of high-confidence β-TrCP substrates and implicating this already well-studied E3 ligase in several new biological processes. Our work highlights the use of BioID as a complementary approach for the identification of E3 targets in living cells.

Acknowledgments—We thank T Srikumar for outstanding technical assistance, S Cheung for FBXW11 cells, and we are extremely grateful to PR Baker and RJ Chalkley for assistance with migrating our mass spectrometry data to MS-Viewer (ProteinProspector). A-CG holds the Canada Research Chair (CRC) in Functional Proteomics, SA holds the CRC in Functional Architecture of Signal Transduction, and BR holds the CRC in Proteomics and Molecular Medicine.

* This project was supported by National Science and Engineering Research Council of Canada grants RGPIN-2014-06434 and RGPAS-462169 to A-CG, and Canadian Institutes of Health Research operating grants to SA (MOP-84273) and BR (MOP-130340).

Ⓢ This article contains supplemental Figs. S1 to S4, Tables S1 to S4, and Movie S1.

¶¶ These authors contributed equally.

§§ To whom correspondence should be addressed: Princess Margaret Cancer Centre, 101 College Street, Toronto, ON M5G 1L7, Canada. Tel.: 416.581.7478; E-mail: brian.raught@uhnres.utoronto.ca.

REFERENCES

1. Varshavsky, A. (2012) The ubiquitin system, an immense realm. *Annu. Rev. Biochem.* **81,** 167–176
2. Hershko, A., and Ciechanover, A. (1998) The ubiquitin system. *Annu. Rev. Biochem.* **67,** 425–479
3. Scheffner, M., and Staub, O. (2007) HECT E3s and human disease. *BMC Biochem.* **8,** S6
4. Jiang, Y. H., and Beaudet, A. L. (2004) Human disorders of ubiquitination and proteasomal degradation. *Curr. Opin. Pediar.* **16,** 419–426
5. Persaud, A., and Rotin, D. (2011) Use of proteome arrays to globally identify substrates for E3 ubiquitin ligases. *Methods Mol. Biol.* **759,** 215–224
6. Rual, J. F., Venkatesan, K., Hao, T., Hirozane-Kishikawa, T., Dricot, A., Li, N., Berriz, G. F., Gibbons, F. D., Dreze, M., Ayivi-Guedehoussou, N., Klitgord, N., Simon, C., Boxem, M., Milstein, S., Rosenberg, J., Goldberg, D. S., Zhang, L. V., Wong, S. L., Franklin, G., Li, S., Albala, J. S., Lim, J., Fraughton, C., Llamosas, E., Cevik, S., Bex, C., Lamesch, P., Sikorski, R. S., Vandenhaute, J., Zoghbi, H. Y., Smolyar, A., Bosak, S., Sequerra, R., Doucette-Stamm, L., Cusick, M. E., Hill, D. E., Roth, F. P., and Vidal, M. (2005) Towards a proteome-scale map of the human protein-protein interaction network. *Nature* **437,** 1173–1178
7. Zhuang, M., Guan, S., Wang, H., Burlingame, A. L., and Wells, J. A. (2013) Substrates of IAP ubiquitin ligases identified with a designed orthogonal E3 ligase, the NEDDylator. *Mol. Cell* **49,** 273–282
8. Yen, H. C., and Elledge, S. J. (2008) Identification of SCF ubiquitin ligase substrates by global protein stability profiling. *Science* **322,** 923–929
9. Hor, S., Ziv, T., Admon, A., and Lehner, P. J. (2009) Stable isotope labeling by amino acids in cell culture and differential plasma membrane proteome quantitation identify new substrates for the MARCH9 transmembrane E3 ligase. *Mol. Cell. Proteomics* **8,** 1959–1971
10. Roux, K. J., Kim, D. I., Raida, M., and Burke, B. (2012) A promiscuous biotin ligase fusion protein identifies proximal and interacting proteins in mammalian cells. *J. Cell Biol.* **196,** 801–810
11. Kwon, K., Streaker, E. D., and Beckett, D. (2002) Binding specificity and the ligand dissociation process in the E. coli biotin holoenzyme synthetase. *Protein Sci.* **11,** 558–570
12. Comartin, D., Gupta, G. D., Fussner, E., Coyaud, E., Hasegan, M., Archinti, M., Cheung, S. W., Pinchev, D., Lawo, S., Raught, B., Bazett-Jones, D. P., Luders, J., and Pelletier, L. (2013) CEP120 and SPICE1 cooperate with CPAP in centriole elongation. *Curr. Biol.* **23,** 1360–1366
13. Firat-Karalar, E. N., Rauniyar, N., Yates, J. R., 3rd, and Stearns, T. (2014) Proximity interactions among centrosome components identify regulators of centriole duplication. *Curr. Biol.* **24,** 664–670
14. Van Itallie, C. M., Aponte, A., Tietgens, A. J., Gucek, M., Fredriksson, K., and Anderson, J. M. (2013) The N and C termini of ZO-1 are surrounded by distinct proteins and functional protein networks. *J. Biol. Chem.* **288,** 13775–13788
15. Van Itallie, C. M., Tietgens, A. J., Aponte, A., Fredriksson, K., Fanning, A. S., Gucek, M., and Anderson, J. M. (2014) Biotin ligase tagging identifies proteins proximal to E-cadherin, including lipoma preferred partner, a regulator of epithelial cell-cell and cell-substrate adhesion. *J. Cell Sci.* **127,** 885–895
16. Couzens, A. L., Knight, J. D., Kean, M. J., Teo, G., Weiss, A., Dunham, W. H., Lin, Z. Y., Bagshaw, R. D., Sicheri, F., Pawson, T., Wrana, J. L., Choi, H., and Gingras, A. C. (2013) Protein interaction network of the Mammalian hippo pathway reveals mechanisms of kinase-phosphatase interactions. *Sci. Signal.* **6,** rs15
17. Willems, A. R., Schwab, M., and Tyers, M. (2004) A hitchhiker's guide to the cullin ubiquitin ligases: SCF and its kin. *Biochim. Biophys. Acta* **1695,** 133–170
18. Kanarek, N., and Ben-Neriah, Y. (2012) Regulation of NF-kappaB by ubiquitination and degradation of the IkappaBs. *Immunol. Rev.* **246,** 77–94
19. Stamos, J. L., and Weis, W. I. (2013) The beta-catenin destruction complex. *Cold Spring Harb Perspect Biol* 5:a007898
20. Zhao, B., Li, L., Tumaneng, K., Wang, C. Y., and Guan, K. L. (2010) A coordinated phosphorylation by Lats and CK1 regulates YAP stability through SCF(beta-TRCP). *Genes Dev.* **24,** 72–85
21. Frescas, D., and Pagano, M. (2008) Deregulated proteolysis by the F-box proteins SKP2 and beta-TrCP: tipping the scales of cancer. *Nat. Rev. Cancer* **8,** 438–449
22. Winston, J. T., Strack, P., Beer-Romero, P., Chu, C. Y., Elledge, S. J., and Harper, J. W. (1999) The SCFbeta-TRCP-ubiquitin ligase complex asso-

ciates specifically with phosphorylated destruction motifs in IkappaBalpha and beta-catenin and stimulates IkappaBalpha ubiquitination in vitro. *Genes Dev.* **13,** 270–283
23. Heckman, K. L., and Pease, L. R. (2007) Gene splicing and mutagenesis by PCR-driven overlap extension. *Nat. Protoc.* **2,** 924–932
24. Kessner, D., Chambers, M., Burke, R., Agus, D., and Mallick, P. (2008) ProteoWizard: open source software for rapid proteomics tools development. *Bioinformatics* **24,** 2534–2536
25. Craig, R., and Beavis, R. C. (2004) TANDEM: matching proteins with tandem mass spectra. *Bioinformatics* **20,** 1466–1467
26. Pedrioli, P. G. (2010) Trans-proteomic pipeline: a pipeline for proteomic analysis. *Methods Mol. Biol.* **604,** 213–238
27. Liu, G., Zhang, J., Larsen, B., Stark, C., Breitkreutz, A., Lin, Z. Y., Breitkreutz, B. J., Ding, Y., Colwill, K., Pasculescu, A., Pawson, T., Wrana, J. L., Nesvizhskii, A. I., Raught, B., Tyers, M., and Gingras, A. C. (2010) ProHits: integrated software for mass spectrometry-based interaction proteomics. *Nat. Biotechnol.* **28,** 1015–1017
28. Choi, H., Larsen, B., Lin, Z. Y., Breitkreutz, A., Mellacheruvu, D., Fermin, D., Qin, Z. S., Tyers, M., Gingras, A. C., and Nesvizhskii, A. I. (2011) SAINT: probabilistic scoring of affinity purification-mass spectrometry data. *Nat. Methods* **8,** 70–73
29. Teo, G., Liu, G., Zhang, J., Nesvizhskii, A. I., Gingras, A. C., and Choi, H. (2014) SAINTexpress: improvements and additional features in Significance Analysis of INTeractome software. *J. Proteomics* **100,** 37–43
30. Baker, P. R., and Chalkley, R. J. (2014) MS-viewer: a web-based spectral viewer for proteomics results. *Mol. Cell. Proteomics* **13,** 1392–1396
31. Tsuchiya, Y., Morita, T., Kim, M., Iemura, S., Natsume, T., Yamamoto, M., and Kobayashi, A. (2011) Dual regulation of the transcriptional activity of Nrf1 by beta-TrCP- and Hrd1-dependent degradation mechanisms. *Mol. Cell. Biol.* **31,** 4500–4512
32. Kean, M. J., Couzens, A. L., and Gingras, A. C. (2012) Mass spectrometry approaches to study mammalian kinase and phosphatase associated proteins. *Methods* **57,** 400–408
33. Hart, M., Concordet, J. P., Lassot, I., Albert, I., del los Santos, R., Durand, H., Perret, C., Rubinfeld, B., Margottin, F., Benarous, R., and Polakis, P. (1999) The F-box protein beta-TrCP associates with phosphorylated beta-catenin and regulates its activity in the cell. *Curr. Biol.* **9,** 207–210
34. Kitagawa, M., Hatakeyama, S., Shirane, M., Matsumoto, M., Ishida, N., Hattori, K., Nakamichi, I., Kikuchi, A., and Nakayama, K. (1999) An F-box protein, FWD1, mediates ubiquitin-dependent proteolysis of beta-catenin. *EMBO J.* **18,** 2401–2410
35. Latres, E., Chiaur, D. S., and Pagano, M. (1999) The human F box protein beta-Trcp associates with the Cul1/Skp1 complex and regulates the stability of beta-catenin. *Oncogene* **18,** 849–854
36. Wu, C., and Ghosh, S. (1999) beta-TrCP mediates the signal-induced ubiquitination of IkappaBbeta. *J. Biol. Chem.* **274,** 29591–29594
37. Nesvizhskii, A. I., Keller, A., Kolker, E., and Aebersold, R. (2003) A statistical model for identifying proteins by tandem mass spectrometry. *Anal. Chem.* **75,** 4646–4658
38. Davis, L. I., and Blobel, G. (1986) Identification and characterization of a nuclear pore complex protein. *Cell* **45,** 699–709
39. Rada, P., Rojo, A. I., Chowdhry, S., McMahon, M., Hayes, J. D., and Cuadrado, A. (2011) SCF/{beta}-TrCP promotes glycogen synthase kinase 3-dependent degradation of the Nrf2 transcription factor in a Keap1-independent manner. *Mol. Cell. Biol.* **31,** 1121–1133
40. Li, V. S., Ng, S. S., Boersema, P. J., Low, T. Y., Karthaus, W. R., Gerlach, J. P., Mohammed, S., Heck, A. J., Maurice, M. M., Mahmoudi, T., and Clevers, H. (2012) Wnt signaling through inhibition of beta-catenin degradation in an intact Axin1 complex. *Cell* **149,** 1245–1256
41. Rothballer, A., Schwartz, T. U., and Kutay, U. (2013) LINCing complex functions at the nuclear envelope: what the molecular architecture of the LINC complex can reveal about its function. *Nucleus* **4,** 29–36
42. Taranum, S., Vaylann, E., Meinke, P., Abraham, S., Yang, L., Neumann, S., Karakesisoglou, I., Wehnert, M., and Noegel, A. A. (2012) LINC complex alterations in DMD and EDMD/CMT fibroblasts. *Eur. J. Cell Biol.* **91,** 614–628
43. Wiederhold, K., and Passmore, L. A. (2010) Cytoplasmic deadenylation: regulation of mRNA fate. *Biochem. Soc. Trans.* **38,** 1531–1536
44. Pfaff, J., and Meister, G. (2013) Argonaute and GW182 proteins: an effective alliance in gene silencing. *Biochem. Soc. Trans.* **41,** 855–860
45. Buchan, J. R. (2014) mRNP granules: Assembly, function, and connections with disease. *RNA Biol.* **11,** 1019–1030
46. Eulalio, A., Behm-Ansmant, I., and Izaurralde, E. (2007) P bodies: at the crossroads of post-transcriptional pathways. *Nat. Rev. Mol. Cell Biol.* **8,** 9–22
47. Jousse, C., Oyadomari, S., Novoa, I., Lu, P., Zhang, Y., Harding, H. P., and Ron, D. (2003) Inhibition of a constitutive translation initiation factor 2alpha phosphatase, CReP, promotes survival of stressed cells. *J. Cell Biol.* **163,** 767–775
48. Ron, D., and Harding, H. P. (2007) eIF2alpha phosphorylation in cellular stress responses and disease. In: Mathews, M. B., Sonenberg, N., and Hershey, J. W., eds. *Translational Control in Biology and Medicine*, pp. 345–368, Cold Spring Harbor Laboratory Press, Cold Spring Harbor, NY
49. Harding, H. P., Zhang, Y., Scheuner, D., Chen, J. J., Kaufman, R. J., and Ron, D. (2009) Ppp1r15 gene knockout reveals an essential role for translation initiation factor 2 alpha (eIF2alpha) dephosphorylation in mammalian development. *Proc. Natl. Acad. Sci. U.S.A.* **106,** 1832–1837
50. Scheuner, D., Song, B., McEwen, E., Liu, C., Laybutt, R., Gillespie, P., Saunders, T., Bonner-Weir, S., and Kaufman, R. J. (2001) Translational control is required for the unfolded protein response and in vivo glucose homeostasis. *Mol. Cell* **7,** 1165–1176
51. Meinke, P., Nguyen, T. D., and Wehnert, M. S. (2011) The LINC complex and human disease. *Biochem. Soc. Trans.* **39,** 1693–1697
52. Kandert, S., Luke, Y., Kleinhenz, T., Neumann, S., Lu, W., Jaeger, V. M., Munck, M., Wehnert, M., Muller, C. R., Zhou, Z., Noegel, A. A., Dabauvalle, M. C., and Karakesisoglou, I. (2007) Nesprin-2 giant safeguards nuclear envelope architecture in LMNA S143F progeria cells. *Hum. Mol. Genet.* **16,** 2944–2959
53. Muchir, A., Medioni, J., Laluc, M., Massart, C., Arimura, T., van der Kooi, A. J., Desguerre, I., Mayer, M., Ferrer, X., Briault, S., Hirano, M., Worman, H. J., Mallet, A., Wehnert, M., Schwartz, K., and Bonne, G. (2004) Nuclear envelope alterations in fibroblasts from patients with muscular dystrophy, cardiomyopathy, and partial lipodystrophy carrying lamin A/C gene mutations. *Muscle Nerve* **30,** 444–450
54. Favreau, C., Dubosclard, E., Ostlund, C., Vigouroux, C., Capeau, J., Wehnert, M., Higuet, D., Worman, H. J., Courvalin, J. C., and Buendia, B. (2003) Expression of lamin A mutated in the carboxyl-terminal tail generates an aberrant nuclear phenotype similar to that observed in cells from patients with Dunnigan-type partial lipodystrophy and Emery-Dreifuss muscular dystrophy. *Exp. Cell Res.* **282,** 14–23
55. Stoecklin, G., and Kedersha, N. (2013) Relationship of GW/P-bodies with stress granules. *Adv Exp Med Biol* **768,** 197–211
56. Low, T. Y., Peng, M., Magliozzi, R., Mohammed, S., Guardavaccaro, D., and AJ, R. H. (2014) A systems-wide screen identifies substrates of the SCFbetaTrCP ubiquitin ligase. *Sci Signal* **7,** rs8
57. Kim, T. Y., Siesser, P. F., Rossman, K. L., Goldfarb, D., Mackinnon, K., Yan, F., Yi, X., MacCoss, M. J., Moon, R. T., Der, C. J., and Major, M. B. (2015) Substrate Trapping Proteomics Reveals Targets of the betaTrCP2/FBXW11 Ubiquitin Ligase. *Mol. Cell. Biol.* **35,** 167–181